Early deglaciation of the British-Irish Ice Sheet on the Atlantic shelf northwest of Ireland driven by glacioisostatic depression and high relative sea level

ó Cofaigh, C., Weilbach, K., Lloyd, J., Benetti, S., Callard, L., Purcell, C., Chiverell, R., Dunlop, P., Saher, M., Livingstone, S., Van Landeghem, K., Moreton, S., Clark, C., & Fabel, D. (2019). Early deglaciation of the British-Irish Ice Sheet on the Atlantic shelf northwest of Ireland driven by glacioisostatic depression and high relative sea level. *Quaternary Science Reviews*, *208*, 76-96. https://doi.org/10.1016/j.quascirev.2018.12.022

Link to publication record in Ulster University Research Portal

Published in:
Quaternary Science Reviews

Publication Status:
Published (in print/issue): 15/03/2019

DOI:
10.1016/j.quascirev.2018.12.022

Document Version
Publisher's PDF, also known as Version of record

General rights
Copyright for the publications made accessible via Ulster University's Research Portal is retained by the author(s) and / or other copyright owners and it is a condition of accessing these publications that users recognise and abide by the legal requirements associated with these rights.

Take down policy
The Research Portal is Ulster University's institutional repository that provides access to Ulster's research outputs. Every effort has been made to ensure that content in the Research Portal does not infringe any person's rights, or applicable UK laws. If you discover content in the Research Portal that you believe breaches copyright or violates any law, please contact pure-support@ulster.ac.uk.

Download date: 17/04/2024

Quaternary Science Reviews 208 (2019) 76–96

Contents lists available at ScienceDirect

Quaternary Science Reviews

journal homepage: www.elsevier.com/locate/quascirev

Early deglaciation of the British-Irish Ice Sheet on the Atlantic shelf northwest of Ireland driven by glacioisostatic depression and high relative sea level

Colm Ó Cofaigh [a, *], Kasper Weilbach [a], Jerry M. Lloyd [a], Sara Benetti [b], S. Louise Callard [a], Catriona Purcell [c], Richard C. Chiverrell [d], Paul Dunlop [b], Margot Saher [c], Stephen J. Livingstone [e], Katrien J.J. Van Landeghem [c], Steven G. Moreton [f], Chris D. Clark [e], Derek Fabel [g]

[a] Department of Geography, Durham University, Durham, DH1 3LE, UK
[b] School of Geography and Environmental Sciences, Ulster University, Coleraine, BT52 1SA, Northern Ireland, UK
[c] School of Ocean Sciences, Bangor University, Menai Bridge, UK
[d] Department of Geography, University of Liverpool, Liverpool, UK
[e] Department of Geography, University of Sheffield, Sheffield, S10 2TN, UK
[f] Natural Environment Research Council, Radiocarbon Facility, East Kilbride, Scotland, G75 OQF, UK
[g] Scottish Universities Environmental Research Centre, East Kilbride, Scotland, G75 OQF, UK

ARTICLE INFO

Article history:
Received 2 August 2017
Received in revised form
13 December 2018
Accepted 14 December 2018
Available online 15 February 2019

Keywords:
British-Irish ice sheet
Ireland
Continental shelf
Last glacial maximum
Ice sheet retreat
Radiocarbon dating
Moraines
Glacimarine

ABSTRACT

Understanding the triggers and pace of marine-based ice sheet decay is critical for constraining the future mass loss and dynamic behaviour of marine-based sectors of the large polar ice sheets in Greenland and Antarctica. Numerical models which seek to predict this behaviour need to be calibrated against data from both contemporary and palaeo-ice sheets, and the latter requires accurate reconstruction of former ice sheet extent, dynamics and timing. Marine geophysics, sediment cores, benthic foraminiferal assemblages and radiocarbon dating are used to reconstruct the extent of the last British-Irish Ice Sheet (BIIS), and the timing and style of its retreat on the Atlantic shelf northwest of Ireland. Shelf edge moraines and subglacial till recovered in cores from the outer continental shelf are dated to younger than 26.3 ka cal BP and indicate an extensive ice sheet at the Last Glacial Maximum (LGM) that was grounded to the shelf edge. Nested arcuate moraines record the subsequent episodic retreat of the ice sheet across the shelf. Lithofacies and associated foraminiferal assemblages demonstrate that this retreat occurred in a glacimarine environment as a grounded tidewater margin and that high relative sea level and cold waters prevailed during retreat. Radiocarbon dates indicate that the timing of initial ice sheet retreat from the shelf edge occurred in the interval between 26.3 and 24.8 ka cal BP, during the period of minimum global eustatic sea level, and that the ice sheet had retreated to the mid-shelf by 24.8 ka cal BP. The 'Donegal Bay Moraine', a large moraine at the mouth of Donegal Bay, records a major stillstand and readvance of the ice sheet during deglaciation between 20.2 and 17.9 ka cal BP. Estimated retreat rates of 5.5–35 m a^{-1} across the shelf demonstrate that retreat was slow. It is noteworthy that retreat was initiated in the absence of ocean warming and when eustatic sea level was at a minimum. The sea-level rise that initiated deglaciation from the shelf edge therefore, is inferred to have been a product of local glacio-isostatic crustal depression rather than external forcing. This demonstrates that marine-based sectors of ice sheets can trigger their own demise internally through glacio-isostatic adjustment and it provides an explanation for the early retreat of the BIIS on the Atlantic shelf during the global LGM (gLGM).

© 2019 The Authors. Published by Elsevier Ltd. This is an open access article under the CC BY license (http://creativecommons.org/licenses/by/4.0/).

1. Introduction

Understanding the dynamic behaviour of marine-based sectors of large ice sheets is of considerable importance due to the potential

* Corresponding author.
E-mail address: colm.ocofaigh@durham.ac.uk (C. Ó Cofaigh).

https://doi.org/10.1016/j.quascirev.2018.12.022
0277-3791/© 2019 The Authors. Published by Elsevier Ltd. This is an open access article under the CC BY license (http://creativecommons.org/licenses/by/4.0/).

inherent instability of these ice masses and their impact on sea level (Bamber et al., 2007; Rignot et al., 2010; Joughin et al., 2014). Numerical ice sheet models that seek to predict the future dynamic behaviour of marine-based ice sheets and, in particular, how they will deglaciate in response to a warming climate are often limited by the short time period over which modern observations extend. Such models are strengthened when tested against chronologically, geomorphologically and stratigraphically well-constrained retreat histories extending over centuries to millennia for individual ice sheets and ice sheet sectors (e.g., Lecavalier et al., 2014; Bentley et al., 2014; Stroeven et al., 2016).

The British-Irish Ice Sheet (BIIS) reached its maximum about 27 ka when it was estimated to have been ca. 840,000 km^2 in area, of which ca. 300,000 km^2 was marine-based (Clark et al., 2012), and it was drained by several fast-flowing ice streams (Eyles and McCabe, 1989; Ó Cofaigh and Evans, 2001; Bradwell et al., 2007; Livingstone et al., 2010; C. Clark et al., 2012; Chiverrell et al., 2013). Although the BIIS was relatively small, its proportionately large marine-based area, combined with its location bordering the North Atlantic, an area known to have experienced large-scale climatic and oceanographic changes during the last cold stage, would have meant that it was sensitive to external forcing(s) and thus make it a useful analogue for how marine-influenced ice sheets deglaciate (C. Clark et al., 2012). While there has been well over a century of research on the last BIIS, the majority of this work, with some exceptions (Scourse et al., 1991, 2000; Stoker, 1995), has focused on its terrestrial geological and geomorphological record. In the last decade, however, the application of improved marine geophysical techniques such as multibeam swath bathymetry (e.g., Van Landeghem et al., 2009; Dunlop et al., 2011; Ó Cofaigh et al., 2012) and the compilation of single beam datasets such as OLEX (Bradwell et al., 2008; C. Clark et al., 2012; Sejrup et al., 2016) has accelerated this research on the continental shelves adjoining Ireland and Britain.

In this paper we refer to the global Last Glacial Maximum (gLGM) and local Last Glacial Maximum (lLGM). The term gLGM is used to refer to the period of 26.5–19 ka when eustatic sea level was at a minimum and sheets were at their maximum extent (P. Clark et al., 2009). However, it is accepted that the timing of the maximum extension of individual ice sheets and different sectors of individual ice sheets was variable (e.g., Patton et al., 2016). Hence the term lLGM refers to the period when a specific ice sheet, such as the last British-Irish Ice Sheet (BIIS), reached its maximum extent. The lLGM for the BIIS was attained slightly earlier than the gLGM at 27 ka (C. Clark et al., 2012).

On the continental shelf northwest and west of Ireland several studies have reconstructed ice sheet extent and flow patterns from marine geophysical and geological investigations (Benetti et al., 2010; Dunlop et al., 2010; Ó Cofaigh et al., 2012, 2016a; C. Clark et al., 2012; Peters et al., 2015, 2016; Callard et al., 2018). These studies have provided evidence for shelf-edge terminating, grounded ice. Although presumed to be of lLGM age, direct dating control on the age of the ice sheet advance and timing and rate of retreat across the shelf is limited to two studies: Peters et al. (2016) from offshore western Ireland, to the south of our study area, and Callard et al. (2018) from further to the north in the Malin Sea. On the Atlantic shelf offshore of northwest Ireland Ó Cofaigh et al. (2012) documented a set of well-developed, nested arcuate moraines which extend inshore from the shelf edge to the mouth of Donegal Bay (Fig. 1). These moraines provide compelling evidence for a grounded ice sheet retreating across the shelf but the timing of advance and retreat, the associated drivers and the nature of the depositional environment(s) are unknown. The present paper addresses this through sedimentological and micropalaeontological investigations of a suite of new sediment cores from the shelf (Fig. 1) dated using twenty two AMS radiocarbon dates and constrained by new sub-bottom profiler records. These cores provide potentially the best dated record for any offshore sector of the last BIIS. Together with the sedimentological, micropalaeontological, and seismostratigraphic analyses, they allow us to constrain the timing of ice sheet advance to the Atlantic shelf edge offshore of northwest Ireland and its subsequent retreat, describe the depositional environments during deglaciation, and finally, to characterize the drivers forcing retreat across the shelf and in particular to determine the role, if any, of ocean warming in this.

2. Methods

The study area is located between 55° 40′ and 54° 18′ N, and 7° 50′ and 11° 4' W and is about 30,000 km^2 in size (Fig. 1). The shelf edge is located at about 125 m water depth and the low gradient shelf extends for over 100 km to the mouth of Donegal Bay where water depths shallow to less than 80 m.

The multibeam swath bathymetric data included in this paper were collected by the Irish Marine Institute and the Geological Survey of Ireland since 1999 as part of the Irish National Seabed Survey (INSS) and Integrated Mapping for the Sustainable Development of Ireland's Marine Resource (INFOMAR) programmes. These data have already been discussed and published in Benetti et al. (2010) and Ó Cofaigh et al. (2012, 2016a) and no new geomorphological mapping is provided here. However, these data are included to provide a geomorphological context for the seismic records, sediment cores and dating. The swath bathymetry data were acquired during surveys of the continental shelf by the *RV Celtic Explorer* and *RV Celtic Voyager* in the period 2002–2008. The multibeam systems used were a hull-mounted Simrad EM1002S and EM3002 on the Celtic Voyager and an EM1002 on the Celtic Explorer with decimetric vertical and horizontal accuracy that varies from 10 to 50 cm according to water depth. The data are gridded at a cell size of 10, 15 or 20 m on the continental shelf according to depth and data quality.

The sub-bottom profiler data and sediment cores presented in this paper were collected during research cruises to the continental shelf in 2008 and 2014. Cruise CE08 of the *RV Celtic Explorer* in 2008 used the Geological Survey of Ireland 6 m long vibrocorer to collect a suite of ten vibrocores along an east-west transect across the shelf (Table 1 and Fig. 1). A further east-west transect of seventeen cores were collected further to the south in 2014 using the British Geological Survey vibrocorer (also with a 6 m barrel) during cruise JC106 of the *RRS James Cook* (Table 1 and Fig. 1). Core sites targeted the series of arcuate moraines imaged in the multibeam data from the shelf (Fig. 2) and individual sites were picked using data from a hull-mounted Kongsberg SBP120 sub-bottom profiler. The system operates a sweep frequency between 2500 and 6500 kHz, with a depth resolution of 0.3 ms and a maximum penetration depth of about 50 m (depending on the nature of the sediments). The profiles were interpreted using the IHS Kingdom™ software. To convert the two-way travel time to depth estimates an average p-wave velocity of 1620 ms^{-1}, measured from sediment cores using a Multi-Sensor Core Logger (MSCL) was used.

Following recovery the sediment cores were cut into 1 m long sections. They were then split and information was recorded on grain size, sedimentary and deformation structures, colour, sorting, bed contacts, clast abundance, clast shape and macrofaunal content. Measurement of sediment shear strength in kPa was recorded using a Torvane. The cores were stored on ship and subsequently in Durham University at +4 °C. Additional information on sedimentary structures was obtained from the post-cruise examination of x-radiographs of the sediment cores. The x-radiographs were created using a GEOTEK MSCL-XCT scanner.

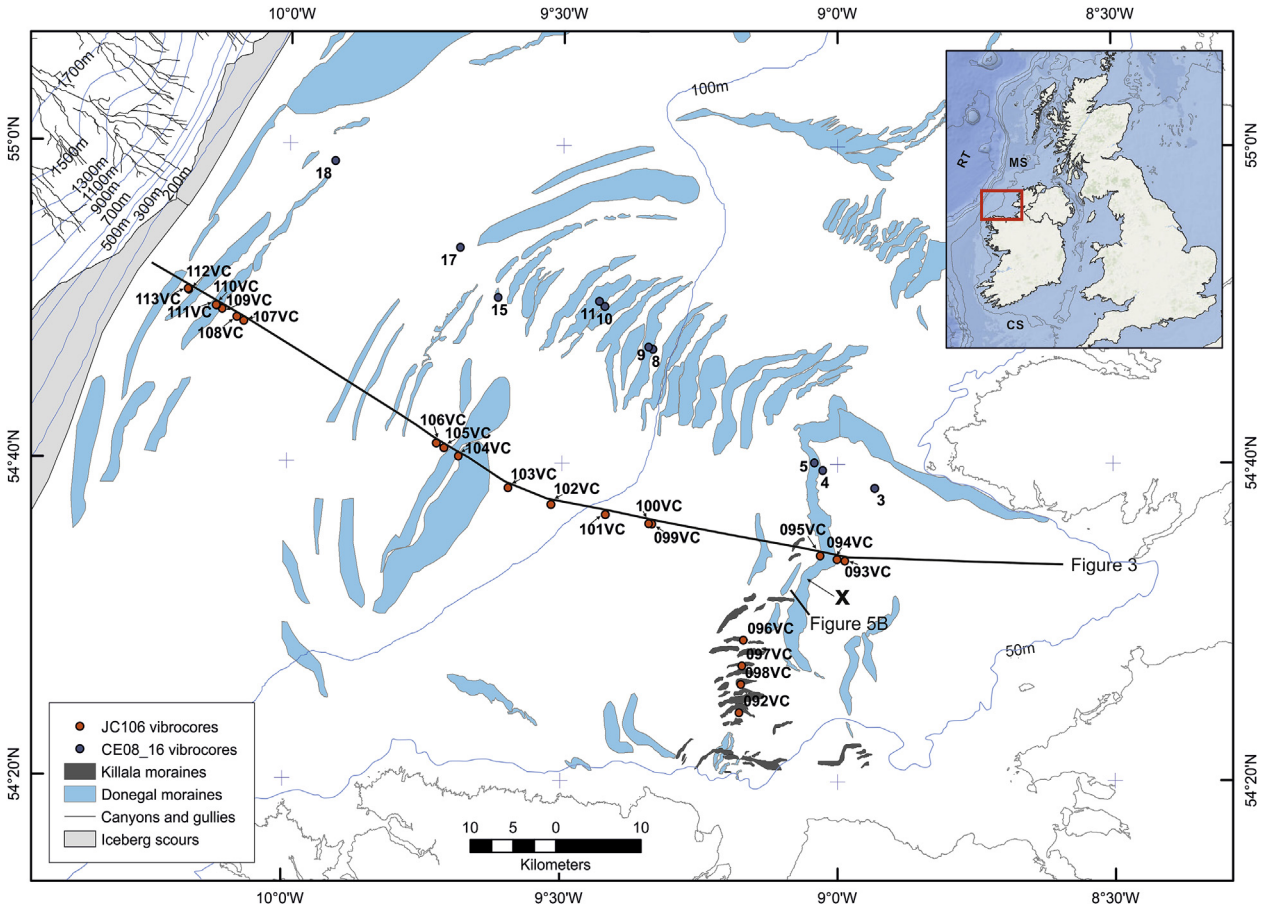

Fig. 1. Continental shelf offshore of northwest Ireland showing numbered core locations and the location of seismic profiles (shown in Figs. 3 and 5). JC106 (RRS James Cook) cores shown in red (cores 093VC-113VC; 'southern transect') and CE008 (RV Celtic Explorer) cores shown in blue (cores 3–18; 'northern transect'). Geomorphological interpretation of glacial features on the continental margin (modified from Benetti et al., 2010 and Ó Cofaigh et al., 2012) is also shown. The location of the 'Donegal Bay Moraine' is arrowed ("X"). Inset map shows locaton of study area offshore northwest Ireland. Labels on inset map: CS = Celtic Sea, MS = Malin Sea, RT = Rockall Trough. (For interpretation of the references to colour in this figure legend, the reader is referred to the Web version of this article.)

Samples of marine carbonate (typically single or broken valves) and benthic foraminifera were picked from the cores for radiocarbon dating. A total of 22 radiocarbon dates were acquired during the course of this study. Sampling typically targeted lithofacies boundaries or, where the cores actually bottomed out in deglacial sediment, the base of the core in order to obtain a minimum age constraint on the timing of ice sheet retreat. Samples were dated at the Natural Environment Research Council (NERC) Radiocarbon Facility (NRCF-East Kilbride). The radiocarbon dates were corrected for isotopic fractionation and a BRITICE-CHRONO specific full process background of 0.30 ± 0.01 pMC (percent modern carbon). They were calibrated with OxCal 4.2 (Bronk Ramsey, 2009) using the Marine13 ^{14}C calibration curve (Reimer et al., 2013), which has an in-built marine reservoir correction of 400 years. Additionally, ΔR values of 0, 300, and 700 years were used (Table 2.) to simulate the possible range of the marine radiocarbon reservoir effect that may have prevailed in the North Atlantic during the demise of the British-Irish Ice Sheet and which is poorly constrained (e.g. Wanamaker et al., 2012). For clarity, only the calibrated ages with ΔR = 0 (±2 sigma) are used in the text.

Micropalaeontological analysis on foraminifera was conducted on a total of 63 samples from six sediment cores. Two cores were sampled at 16 cm increments through the entire core length, and another four cores were sampled at varying increments across key changes in lithofacies. For each sample 5–7 ml of sediment was wet sieved through 500 μm and 63 μm sieves. Foraminifera were then dry picked from the 63 to 500 μm fraction of sediment using a Leica MZ75 binocular microscope. Large bulk samples were split to obtain samples with 300 foraminifera tests. Individuals were counted and identified to species level and species counts were then converted to percentages.

3. Geophysical data

3.1. Seafloor geomorphology

3.1.1. Description

Multibeam-swath bathymetric data extending from the mouth of Donegal Bay to the continental shelf edge show a series of prominent NE to SW aligned and nested sediment ridges on the shelf (Fig. 2) (Ó Cofaigh et al., 2012, 2016a). Most of the ridges are arcuate in planform although some of the longer ridges have relatively straight sections. The most prominent ridge occurs at the mouth of Donegal Bay (Fig. 2). This large ridge (termed hereafter the 'Donegal Bay Moraine') is 35 km long, up to 2.5 km wide and 15 m high. The ridge is generally sharp-crested but towards its northern end it has a broader, flatter profile. Further offshore and extending across the mid-shelf is a suite of closely-spaced, arcuate ridges. The outer ridges in this sequence are 0.2–3.5 km wide, 1–4 m high, and are lobate and nested. Morphologically the ridges tend to be asymmetric with a gentler seaward (NW) side and a steeper landward (SE) side.

Table 1
Site information on sediment cores from Donegal Bay and the adjoining shelf.

Core name	Location	Water depth (m)	Recovery (m)
CE08-003	54.6415° N, 8.9324° W	88	5.12
CE08-004	54.6601° N, 9.0260° W	82	2.75
CE08-005	54.6679° N, 9.0414° W	67	6.9
CE08-008	54.7869° N, 9.3348° W	90	3.22
CE08-009	54.7891° N, 9.3428° W	90	0.74
CE08-010	54.8316° N, 9.4233° W	97	5.78
CE08-011	54.8370° N, 9.4332° W	95	1.39
CE08-015	54.8403° N, 9.6179° W	99	2.78
CE08-017	54.8926° N, 9.6872° W	122	1.3
CE08-018	54.9822° N, 9.9172° W	122	1.0
JC106-092VC	54° 24.331′N, 9° 10.608′W	75	2.7
JC106-093VC	54° 33.898′N, 8° 59.177′W	81.6	3.55
JC106-094VC	54° 34.009′N, 9° 0.049′W	75.6	0.86
JC106-095VC	54° 34.238′N, 9° 1.832′W	77.6	2.31
JC106-096VC	54° 28.913′N, 9° 10.181′W	75	3.06
JC106-097VC	54° 27.287′N, 9° 10.322′W	75	4.71
JC106-098VC	54° 26.115′N, 9° 10.446′W	75	0
JC106-099VC	54° 36.218′N, 9° 20.139′W	99	4.75
JC106-100VC	54° 36.243′N, 9° 20.496′W	99	4.97
JC106-101VC	54° 36.784′N, 9° 25.241′W	100	5.65
JC106-102VC	54° 37.407′N, 9° 31.134′W	90.5	2.52
JC106-103VC	54° 38.438′N, 9° 35.833′W	100	1.49
JC106-104VC	54° 40.393′N, 9° 41.239′W	102	0.94
JC106-105VC	54° 40.917′N, 9° 42.838′W	108	5.82
JC106-106VC	54° 41.202′N, 9° 43.656′W	105	3.94
JC106-107VC	54° 48.783′N, 10° 4.829′W	117	1.22
JC106-108VC	54° 49.023′N, 10° 5.607′W	119	0.45
JC106-109VC	54° 49.521′N, 10° 7.189′W	120	0
JC106-110VC	54° 49.714′N, 10° 7.808′W	122.7	0.31
JC106-111VC	54° 49.739′N, 10° 7.881′W	123	0.3
JC106-112VC	54° 50.708′N, 10° 10.882′W	125	1
JC106-113VC	54° 50.742′N, 10° 10.98′W	125	0.23

A further set of ridges extends northwards from the mouth of Killala Bay off the north Mayo coast. They are predominantly aligned east–west, are straight to arcuate in planform, 0.7–3 km long, 0.1–0.7 km wide and 2.5–5 m high. Termed the 'Killala Moraines' (Fig. 1) (Benetti et al., 2010; Ó Cofaigh et al., 2012). They are superimposed on top of the Donegal Bay Moraine, and are therefore younger.

3.1.2. Interpretation

The arcuate sediment ridges on the shelf have been interpreted as moraines formed at the margin of a grounded Irish Ice Sheet (see Ó Cofaigh et al., 2012, 2016a). The largest moraines are positioned along the shelf edge and record the outermost extent of shelf glaciation. Further inshore the moraines are smaller, closely spaced, nested and often arcuate in planform and are asymmetric with steeper ice-contact faces. They record episodic, ice-marginal recession, punctuated by minor readvances or oscillations (Ó Cofaigh et al., 2012, 2016a). Such oscillations are consistent with localised bifurcation of the ridges. The arcuate outer moraines record the former presence of a large ice lobe which extended over 80 km from the mouth of Donegal Bay to the shelf edge and was up to approximately 120 km wide. The moraines indicate that at the glacial maximum the BIIS margin was grounded at the shelf break (Ó Cofaigh et al., 2012). The prominent Donegal Bay Moraine (Fig. 2) has been interpreted variously as a readvance limit formed during the Killard Point Stadial (J. Clark et al., 2009) or a recessional moraine formed during deglaciation (Ó Cofaigh et al., 2012). The age of this moraine is discussed further below. Based on their superimposition on top of the Donegal Bay Moraine, the smaller east-west ridges are interpreted as a series of moraines that record a late-stage, lobate, readvance of ice into Donegal Bay from the south (Benetti et al., 2010; Ó Cofaigh et al., 2012).

3.2. Acoustic facies

3.2.1. Description

Fig. 3 shows a sub-bottom profile line that extends eastwards from the shelf edge to Donegal Bay. The profile can be divided into four sections: (1) Outer shelf and shelf break; (2) Mid-shelf; (3) Donegal Bay Moraine; and (4) Inner shelf (Fig. 3). The outer shelf contains a prominent moraine that is visible on both the multibeam (see above) and sub-bottom profiler data (Figs. 2 and 3). The mid-

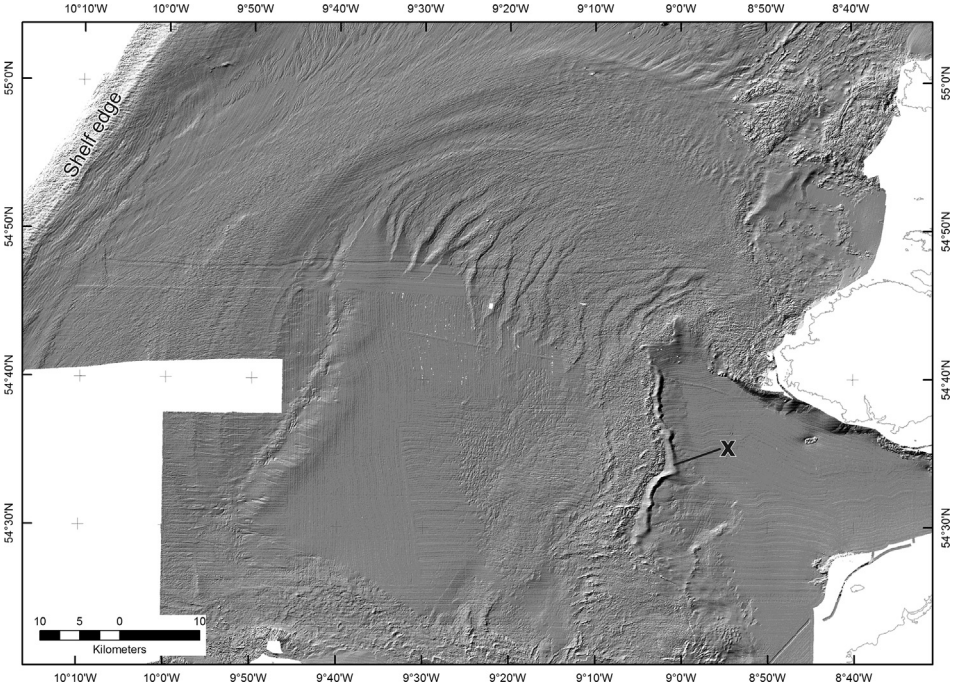

Fig. 2. Shaded relief image of arcuate moraines in Donegal Bay and the adjoining shelf. The Donegal Bay Moraine (see text) is labelled 'X'.

Table 2
Radiocarbon dates from marine sediment cores on the continental shelf offshore of northwest Ireland. In the Notes column, "DBM" = Donegal Bay Moraine. Radiocarbon ages were calibrated using OxCal 4.2, web interface build number 94 (Bronk Ramsey, 2009) with the Marine13^{14}C - modelled ocean average calibration curve (Reimer et al., 2013).

Sample ID	Lab code	Sample depth (cm)	Sample material	Conventional ^{14}C age (yr BP) ± 1σ	Calibrated age (cal yr BP) ± 1σ. ΔR = 0 yr.	Calibrated age (cal yr BP) ± 1σ. ΔR = 300 yr.	Calibrated age (cal yr BP) ± 1σ. ΔR = 700 yr.	Notes
T6-095VC-128	SUERC-58402	128	Shell fragment	13527 ± 39	15759 ± 190	15283 ± 171	14518 ± 329	From massive glacimarine mud, 95VC, DBM
T6-095VC-175.5	SUERC-58403	175.5	Shell fragment	13516 ± 38	15740 ± 192	15266 ± 161	14493 ± 319	From laminated glacimarine mud, 95VC, DBM
T6-095VC-209	SUERC-63557	209	Mixed benthic foraminifera	14760 ± 45	17493 ± 176	17084 ± 212	16465 ± 220	From laminated glacimarine mud, 95VC, DBM
T6-099VC-474	UCIAMS-164429	474	Mixed benthic foraminifera	17180 ± 80	20239 ± 239	19870 ± 245	19394 ± 233	From interbedded laminated & massive glacimarine mud, 99VC base, mid-shelf
T6-101VC-548-551	UCIAMS-164431	548–551	Mixed benthic foraminifera	20110 ± 120	23733 ± 319	23361 ± 353	22885 ± 353	From laminated glacimarine mud, 101VC base, mid-shelf
T6-102VC-72	SUERC-59510	72	Shell fragment	16692 ± 45	19669 ± 186	19300 ± 190	18835 ± 106	From laminated glacimarine mud 102VC, mid-shelf
T6-102VC-247	UCIAMS-164437	247	Mixed benthic foraminifera	21000 ± 110	24804 ± 388	24387 ± 339	23939 ± 300	From laminated glacimarine mud, 102VC base, mid-shelf
T6-103VC-145	SUERC-63558	145	Mixed benthic foraminifera	22521 ± 70	26319 ± 247	26031 ± 161	25744 ± 163	From massive sand, 103VC base, mid-shelf
T6-105VC-572	UCIAMS-164438	572	Mixed benthic foraminifera	19290 ± 90	22745 ± 259	22460 ± 194	22052 ± 267	From interstratified sands and muds, 105VC base, mid-shelf
T6-106VC-389	UCIAMS-164435	389	Mixed benthic foraminifera	18850 ± 90	22307 ± 237	22007 ± 274	21484 ± 310	From massive glacimarine mud, 106VC base, mid-shelf
T6-112VC-51	SUERC-63584	51	Shell fragment	22582 ± 67	26382 ± 257	26082 ± 178	25791 ± 153	From massive diamicton (till), 112VC, outer shelf
T6-112VC-59.5	SUERC-63585	59.5	Shell fragment	22572 ± 71	26372 ± 259	26074 ± 180	25783 ± 159	From massive diamicton (till), 112VC, outer shelf
T6CE08-018-CC	UCIAMS-133552	core catcher	Mixed benthic foraminifera	20170 ± 90	23796 ± 267	23436 ± 310	22964 ± 308	From laminated sand, base, CE08-018, outer shelf
T6CE08-015-272	SUERC-47518	272	Shell fragment	12495 ± 40	13976 ± 137	13645 ± 151	13272 ± 104	From massive sand, CE08-015, mid- shelf
T6CE08-010-573	SUERC-58324	573–578	Mixed benthic foraminifera	15263 ± 43	18063 ± 167	17743 ± 176	17241 ± 196	From massive glacimarine diamicton CE08-010, mid-shelf
T6CE08-010-471	UCIAMS-133551	471–478	Mixed benthic foraminifera	13205 ± 35	15250 ± 145	14735 ± 339	13987 ± 131	From massive sand, CE08-010, mid- shelf
T6CE08-004-264	SUERC-47522	264–273	Mixed benthic foraminifera	15130 ± 44	17918 ± 161	17584 ± 178	17036 ± 212	From laminated glacimarine mud, CE08-004, inner shelf, inshore of DBM
T6CE08-004-217	SUERC-47517	217	Shell fragment	11555 ± 39	13030 ± 139	12730 ± 110	12371 ± 208	From massive sand, CE08-004, inner shelf, inshore of DBM
T6CE08-003-493	UCIAMS-133550	493–499	Mixed benthic foraminifera	11345 ± 30	12800 ± 118	12595 ± 76	11981 ± 157	From laminated glacimarine mud, CE08-003, inner shelf
T6CE08-003-477	SUERC-47516	477	Single valve, *Macoma calcarea*	11219 ± 39	12702 ± 102	12472 ± 157	11725 ± 270	From laminated glacimarine mud, CE08-003, inner shelf
T6CE08-003-466	SUERC-47515	466	Single valve, *Macoma calcarea*	11091 ± 38	12622 ± 80	12266 ± 220	11469 ± 247	From laminated glacimarine mud, CE08-003, inner shelf
T6CE08-003-387	SUERC-47514	387	Shell fragment	10802 ± 38	12284 ± 218	11683 ± 274	11107 ± 112	From laminated glacimarine mud, CE08-003, inner shelf

shelf extends ca. 35–40 km to the Donegal Bay Moraine with a water depth of about 100 m. The Donegal Bay Moraine consists of two parts: a 2.5 km wide "eastern ridge" with a steep inner slope and a western, outer ridge that has an irregular surface. The inner shelf extends eastwards from the Donegal Bay Moraine for approximately 25 km to the shallow coastal area. . Three acoustic facies are recognised along this sub-bottom profile (Figs. 3 and 4).

3.2.1.1. Facies A. Facies A is acoustically structureless and constitutes the lowermost acoustic facies imaged in this study. It occurs across the shelf but is best seen in records from the mid- and inner shelf. It has a pronounced sub-seafloor topography within the mid-shelf basin where it comprises a series of what appear to be buried ridges 20–25 m high and 0.5–1 km wide (Figs. 3 and 4). The buried ridges can be seen across the mid-shelf and become larger with

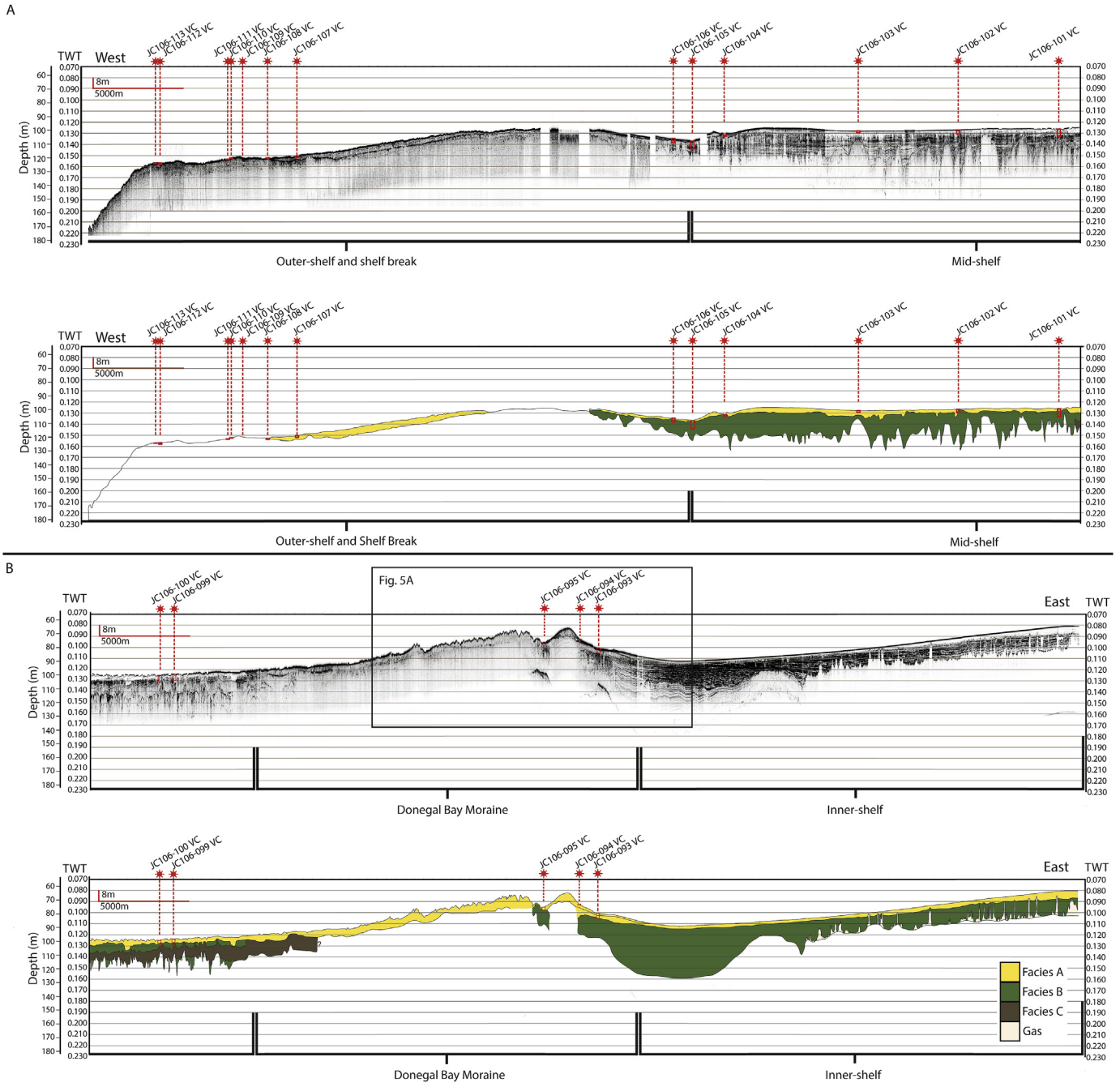

Fig. 3. Seismic profile (and associated interpretation) extending eastwards from the continental shelf edge to Donegal Bay showing the location of sediment cores. The location of the seismic profile is shown in Fig. 1. The profile is split into two parts. Part A covers the shelf edge to mid-shelf, and the eastwards continuation of the profile is shown underneath in part B which covers the mid-to inner-shelf.

increasing distance to the west. Inter-ridge areas are commonly infilled by acoustic Facies B (Fig. 4). On the west side of the Donegal Bay Moraine, Facies A is interbedded with the acoustically laminated sediments of Facies B (Fig. 4). Cores from Facies A (CE08-008, JC106-108, JC106-110, JC106-111, JC106-112) recovered stiff, massive, matrix-supported diamicton (Lithofacies 1 – see below).

3.2.1.2. Facies B. Facies B overlies unconformably Facies A and is characterised by well-developed, acoustic stratification with frequent parallel and sub-parallel, moderate amplitude reflectors (Figs. 3 and 4). It is particularly prominent on the inner-shelf where it onlaps Facies A and reaches a thickness of at least 40 m (Fig. 3). On the mid-shelf Facies B attains a thickness of ca. 25 m and infills the depressions between the topographic highs of Facies A, in some cases on-lapping the basin sides. (Fig. 3). Fig. 5 shows the acoustic characteristics of the Donegal Bay Moraine. On the eastern side of the moraine, Facies B is markedly contorted and in places has a chaotic appearance with only traces of the original reflectors visible (Fig. 5A, B).

Within the Donegal Bay Moraine itself acoustic penetration is reduced but traces of Facies B are imaged beneath the eastern ridge and also between the eastern and western ridges (Fig. 5). In the latter location Facies B appears locally contorted (Fig. 5A). Facies B thickens westwards from the Donegal Bay Moraine and appears to

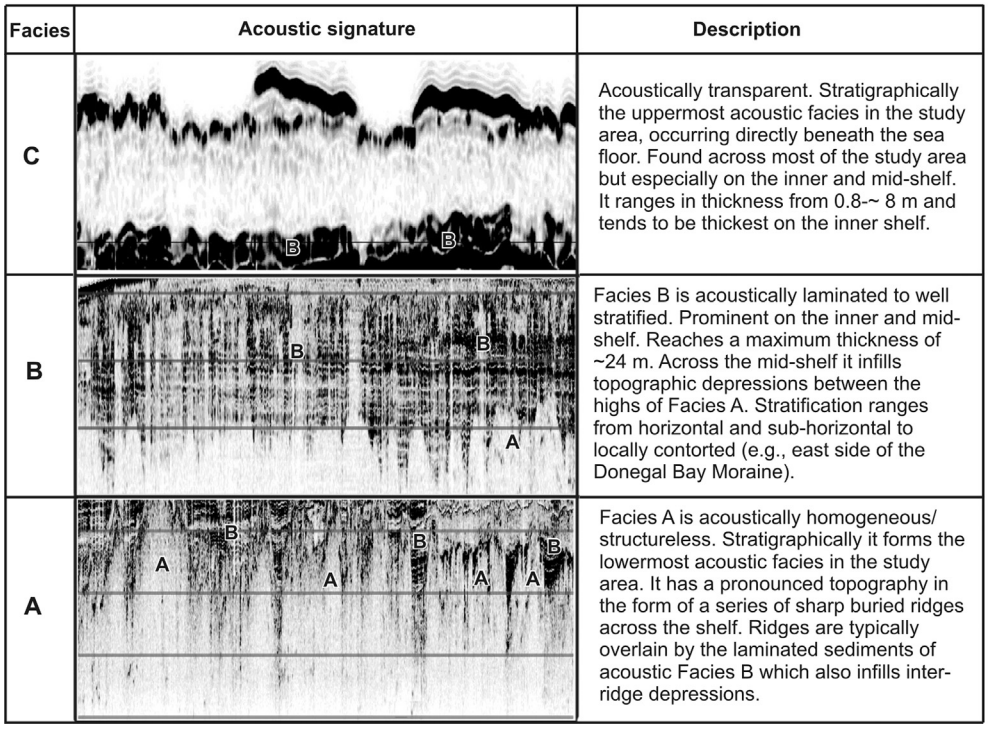

Fig. 4. Acoustic facies observed in sub-bottom profiles from the study area.

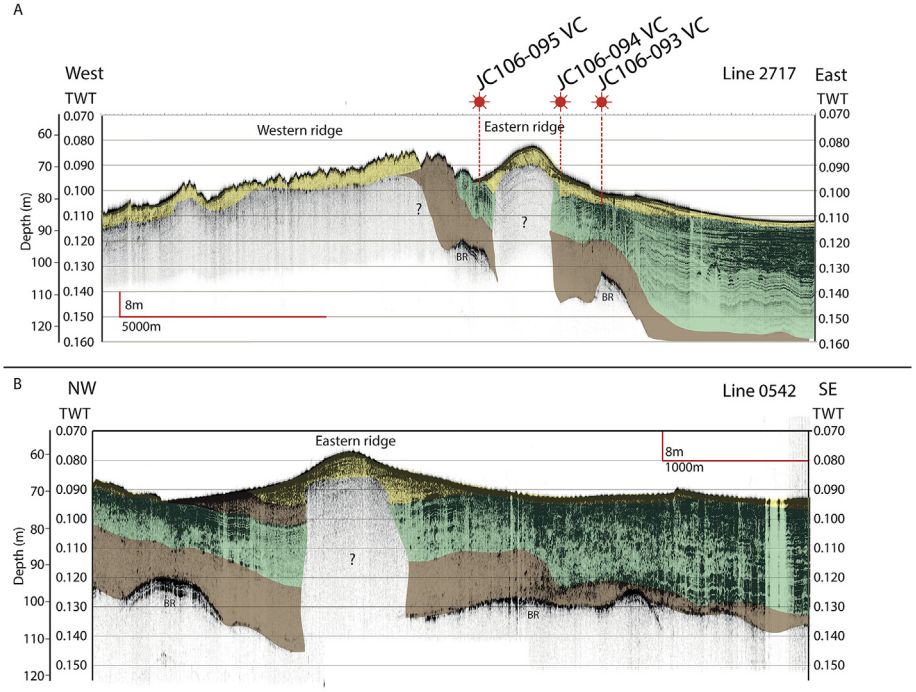

Fig. 5. Examples of internal structure of the Donegal Moraine. Note the contorted stratified acoustic sediments on southeast side of eastern ridge in both profiles. The location of the upper profile (A) is shown in Fig. 3, and that of the lower profile (B) is shown in Fig. 1.

terminate on the outer shelf moraine, although the base of the facies is not always visible due to acoustic attenuation. Sediment cores from Facies B recovered laminated and massive muds (CE08-003, JC106-95, JC106-99, JC106-100, JC106-101, JC106-102, JC106-105) (Lithofacies 2 and 3 – see below).

3.2.1.3. Facies C. Facies C is acoustically transparent to structureless (Figs. 3 and 4). Stratigraphically it is the uppermost acoustic facies and typically immediately underlies the seafloor reflector. It is prominent on the mid- and inner-shelf, both inshore and offshore of the Donegal Bay Moraine and also occurs on the outer shelf but disappears close to the shelf break (Fig. 3). On the mid-shelf the

thickness of Facies C ranges from ca. 4.5–7 m and is up to 8 m thick on the inner-shelf. Sediment cores from Facies C recovered massive and horizontally bedded gravels (clast- and matrix-supported) and sands often containing a 'shell hash' of broken and whole bivalves (Lithofacies 5–8 – see below).

3.2.2. Interpretation

3.2.2.1. Facies A. Facies A is stratigraphically the lowermost acoustic facies in this study and it forms a series of buried bathymetric highs across the shelf. These include the Donegal Bay Moraine and outer shelf moraine but on the mid-shelf most of the moraines are lower in amplitude and are buried by Facies B; hence they have no seafloor expression and are only visible in the sub-bottom profile (Fig. 3). Cores from this facies recovered stiff, matrix-supported massive diamicton (see below). Based on its lack of internal structure, its unconformable upper surface, its composition as a stiff diamicton and its geomorphological expression as a series of topographic highs, either buried or visible above the seafloor, we infer that Facies A is a diamicton of either subglacial and/or ice-marginal origin which forms a series of shelf moraines (cf. Forwick and Vorren, 2011; Hogan et al., 2016; Graham and Hodgson, 2016). In this interpretation the infills of acoustically stratified Facies B between the moraine ridges were deposited time-transgressively as the ice sheet retreated across the shelf.

Interbedding of facies A and B on the western (ice distal) side of the Donegal Bay Moraine is inferred to reflect glacigenic sedimentation sourced from an ice margin grounded at the moraine. The interbedding of transparent and laminated acoustic facies suggest subaqueous depositional processes, with Facies A produced by sediment failure and downslope resedimentation of unstable glacigenic sediment from the moraine (cf. Whittington and Niessen, 1997; Forwick and Vorren, 2011; Dowdeswell et al., 2016). Resedimentation of glacigenic sediment is common in ice-proximal glacimarine settings where depositional oversteepening due to high sedimentation rates, combined with disturbance from grounding icebergs and ice-front oscillations, act to trigger mass flows (Lønne, 1995; Powell, 2003).

The prominent seafloor morphology and large size of the Donegal Bay Moraine indicate that it represents a major stillstand and/or ice-marginal oscillation. The latter is suggested by the composite form of the moraine that actually comprises two ridges with the western (outermost) ridge being the older of the two. It is also supported by the presence of heavily contorted Facies B sediments in the eastern side of the moraine which we suggest were glactectonised following their initial subaqueous (see below) deposition. Undeformed, acoustically stratified, conformable sediments of Facies B to the east of the Donegal Bay Moraine were deposited after the ice margin had receded from the moraine into the inner part of Donegal Bay.

3.2.2.2. Facies B. The well-developed stratification and on-lapping geometry of Facies B, combined with sediment core evidence which shows it is composed of laminated and massive muds are consistent with fine-grained sediment input in a subaqueous setting. Such facies have been commonly described from glacimarine environments where they are formed by rain-out from turbid meltwater plumes and iceberg rafting, likely combined with localised deposition from dilute sediment gravity flows (Gilbert et al., 1993; Powell and Domack, 1995; Hogan et al., 2012; Ó Cofaigh et al., 2016b). Facies B tends to infill the depressions between the topographic highs of Facies A rather than drape them and this suggests that emplacement of Facies B was likely time-transgressive and associated with sediment being sourced from the vicinity of the topographic highs.

3.2.2.3. Facies C. Stratigraphically this is the uppermost acoustic facies in the study area and is therefore the youngest. It is acoustically transparent or structureless and occurs beneath the seafloor reflector. Cores from Facies C show that it variably comprises sand and poorly-sorted clast- and matrix-supported gravel, in some cases rich in single and broken bivalve shells. Facies C is interpreted to post-date ice sheet retreat in the bay. The sedimentological evidence for clast-supported gravels and shell hash points to bottom-current winnowing (cf. Howe et al., 2001; Howe, 2006) and Facies C is therefore interpreted largely as a product of post-glacial sedimentation and bottom-current activity (Viana et al., 1998).

4. Sediment cores

4.1. Radiocarbon dates

Twenty two radiocarbon dates were obtained on samples of shells and foraminifera from cores across the shelf (Tables 1 and 2). The dates are shown at their stratigraphic depths on the core logs in Fig. 6. Samples for dating were selected predominantly to constrain the timing of retreat across the shelf but two samples of reworked shell fragments were dated to constrain the maximum age of till formation and thus ice sheet advance on the outer shelf. The conventional radiocarbon and calibrated ages are shown in Table 2.

4.2. Sedimentology

Twenty seven vibrocores from outer Donegal Bay and the adjoining shelf were investigated in this study. Core sites were selected from analysis of the seafloor geomorphological and acoustic stratigraphic data and targeted acoustically stratified sediments (Facies B) in between moraine ridges where possible. Lithofacies were identified and are described stratigraphically from oldest (bottom) to youngest (top). Lithofacies codes are based on Eyles et al. (1983) and outlined in Table 3.

4.2.1. Lithofacies: description

4.2.1.1. Lithofacies 1 – massive, matrix-supported diamicton (Dmm). This lithofacies corresponds to acoustic Facies A. Massive, matrix-supported diamicton was recovered in cores from the mid- and outer-shelf: cores CE08-008, CE08-010, CE08-011, JC106-108VC, JC106-111VC and JC106-112VC. The diamicton is brownish grey in colour and it comprises the basal unit in all of the cores where it is present (Figs. 6 and 7). Recovery of this lithofacies ranged from 0.6 to 2 m. Two sub-facies can be recognised.

Lithofacies 1a comprises stiff, massive, matrix-supported diamicton which in some cores (e.g., 112VC from the outer shelf) contains shell fragments (Figs. 6, 7a and 7b). Shear strengths range from 50 to 220 kPa. The matrix consists of silt and clay with dispersed clasts, mostly up to 2 cm in diameter although occasional clasts up 5 cm in diameter are also observed. Clasts display no preferred orientation on the x-radiographs and are predominantly sub-angular with subsidiary sub-rounded and angular clasts.

Lithofacies 1b was only observed in core CE08-010 where it is the lowermost facies in the core at 578-484 cm (Figs. 6 and 7). Like Lithofacies 1a it comprises a matrix-supported diamicton. However, it differs from Lithofacies 1a in that in places it is locally transitional to a diffusely laminated diamicton (Dml) (567-555 cm depth) with dropstones (Fig. 7b). It also contains marked variations in clast content resulting in subtle transitions from clast-poor to clast-rich diamicton. Clasts within Lithofacies 1b are sub-angular to sub-rounded and are up to pebble size. The upper contact is gradational into massive clast-free sand (Sm). Shear strength in the diamicton ranges from 76 to 48 kPa from 572 to 534 cm, whereas above 534 cm depth, the diamicton is softer with shear strength

Table 3
Lithofacies in cores from Donegal Bay and adjoining shelf (after Eyles et al., 1983).

Lithofacies	Description
Dmm (minor Dml)	Diamict, matrix-supported and massive. Can be divided into two sub-facies. Lithofacies 1a (Dmm) is stiff, massive, contains reworked shells fragments, matrix of silt-clay with dispersed clasts of no apparent preferred orientation. Lithofacies 1b is a massive diamicton (Dmm) that is locally transitional to a diffusely laminated diamicton (Dml) with dropstones. Texturally it ranges from zones of clast-poor to clast-rich diamicton. Well preserved benthic glacimarine foraminiferal assemblage.
Gm	Gravel, clast-supported
Gms	Gravel, matrix-supported
Suf	Sand, normally graded.
Sh	Sand, horizontally-laminated
Sm	Sand, massive
Fl	Mud, laminated.
Fld	Mud, laminated with clasts
Fm	Mud, massive
Fmd	Mud, massive with clasts. Occasionally transitional to Dmm

values ranging from 48 to 31 kPa.

4.2.1.2. Lithofacies 2 – laminated mud (Fl; minor Fld). This lithofacies corresponds to acoustic Facies B. It comprises laminated muds with occasional clasts, usually sub-cm in diameter. It is thickest in cores from the mid-shelf (e.g., JC106-99VC, JC106-100VC, JC106-101VC and JC106-101VC) but also occurs in the lower parts of cores from the inner shelf (JC106-95VC, CE08-04 and CE08-03) (Figs. 6, 7e and 7f). It reaches a maximum thickness of 4.5 m in core JC106-99VC. The muds are soft with typical shear strengths ranging from 10 to 15 kPa. Lamination is imparted by alternating bands of silt or fine sand and grey clay which appear on x-radiographs as alternating light (coarser and less dense) and dark (finer and denser) sediment (Fig. 7e). Lamination is typically horizontal or sub-horizontal and undeformed, apart from occasional contortion and normal faults. Down-warping at core edges is attributed to the coring process. Rare, small, pebble-sized clasts occur within the laminated muds. In several cores (e.g., JC106-100VC and JC106-101VC) the lamination appears rhythmic and the laminae form couplets with a sharp-based, coarser lower lamina (lighter on x-radiographs) grading upwards into the finer (darker) lamina. However, this relationship is not consistent and some finer laminae also have sharp bases. In places the lamination is more stratified with interbedded sands and silty clays (e.g., the lower 1 m of core JC106-105VC). Bounding contacts for this lithofacies are typically abrupt (Fig. 7f).

4.2.1.3. Lithofacies 3 – massive mud and massive diamictic mud (Fm, Fmd). This lithofacies corresponds to acoustic Facies B. It consists of grey and olive-grey massive mud, with (Fmd) or without (Fm) clasts, that is occasionally bioturbated. As in the case of Lithofacies 2 (laminated mud) it is particularly common in cores from the mid-shelf (e.g., cores CE08-010, JC106-100VC, JC106-101VC and JC106-105VC) although it also occurs in cores from the Donegal Bay Moraine (JC106-95VC) and the inner shelf (CE08-003) (Fig. 6). In thickness Lithofacies 3 ranges from a few cm to almost 2 m. In some cores (e.g., CE08-010,352–372 cm depth; JC106-100VC 310–494 cm depth) the massive mud contains sufficient numbers of small clasts to be transitional to massive diamicton although shear strength values are much lower (25 kPa) than is the case with Lithofacies 1a (see above). In core JC106-100VC the massive mud is separated from the overlying laminated mud of Lithofacies 2 by a sharp contact, although thin horizons of massive mud with clasts are interbedded with clast-poor laminated mud for about 10 cm above this contact (Fig. 7f). Although predominantly massive, Lithofacies 3 occasionally shows localised zones of very diffuse lamination/stratification up to a few cm thick.

4.2.1.4. Lithofacies 4 – laminated or stratified sand (Sh). Laminated or stratified sand (Lithofacies 4) was observed in a few cores, primarily from the mid-shelf (Figs. 6 and 7g). Beds of this lithofacies tend to be relatively thin (≤0.2 m). The sediment is clast-poor, and individual laminae range from weak and diffuse to well-developed with sharp boundaries. In some cores laminae may be disturbed or contorted. Lithofacies 4 is relatively thin (≤0.2 m) and either corresponds to acoustic Facies C or B. A correspondence with Facies B is more consistent with the age of this lithofacies which we discuss below.

4.2.1.5. Lithofacies 5 – normally graded sand (Suf). Lithofacies 5–8 correspond to acoustic Facies C. Fining upwards sands were occasionally observed. The sands tend to have sharp bases and range from poorly sorted granular sand that fines upwards into well sorted fine sand, to finer sands that grade upwards to diffusely laminated silty sand (e.g., CE08-03, 430-410 cm depth). Typically normally graded sands have concentrations of broken and fragmented shells and occasional pebbles along their lower boundary or within the lowermost few centimetres.

4.2.1.6. Lithofacies 6 – massive sand (Sm). Massive sand occurs in most of the cores and ranges in thickness from 0.1 m to several metres (Fig. 6). Texturally it ranges from silty to coarse but is usually well sorted. Clast content is variable from granules and pebbles to, occasionally, cobbles. Bounding contacts are usually sharp although in some cores massive sand beds may have sharp lower and upper gradational contacts and are overlain by either laminated or massive muds (e.g., CE08-003, 443-374 cm). In many cores massive sand forms the uppermost lithofacies and caps the stratigraphic sequence (e.g., CE08- 003, CE08-004, CE08-005, CE08-010, CE08-011, JC106-100VC, JC106-106VC) (Fig. 6) and is equivalent to Acoustic Facies C. These capping massive sands contain broken and fragmented shells which are often abundant, and contain clasts from granule to pebble size, either dispersed or arranged in layers 1–3 clasts thick. The massive sand in the top of the cores may display diffuse textural variation. They commonly overlie gravelly facies (Gm and Gms).

4.2.1.7. Lithofacies 7 – clast-supported, massive gravel (Gm). This facies comprises clast-supported gravel which is usually well sorted, massive and contains sub-rounded to rounded clasts (Figs. 6 and 7d). Occasionally it can exhibit a subtle normal grading. Together, lithofacies 6 and 7 often form part of a sequence of sand and gravel facies that are separated by gradational contacts and cap many of the sediment cores from across the shelf. Clast sizes range from granules to pebbles and in some case cobbles. Beds of this

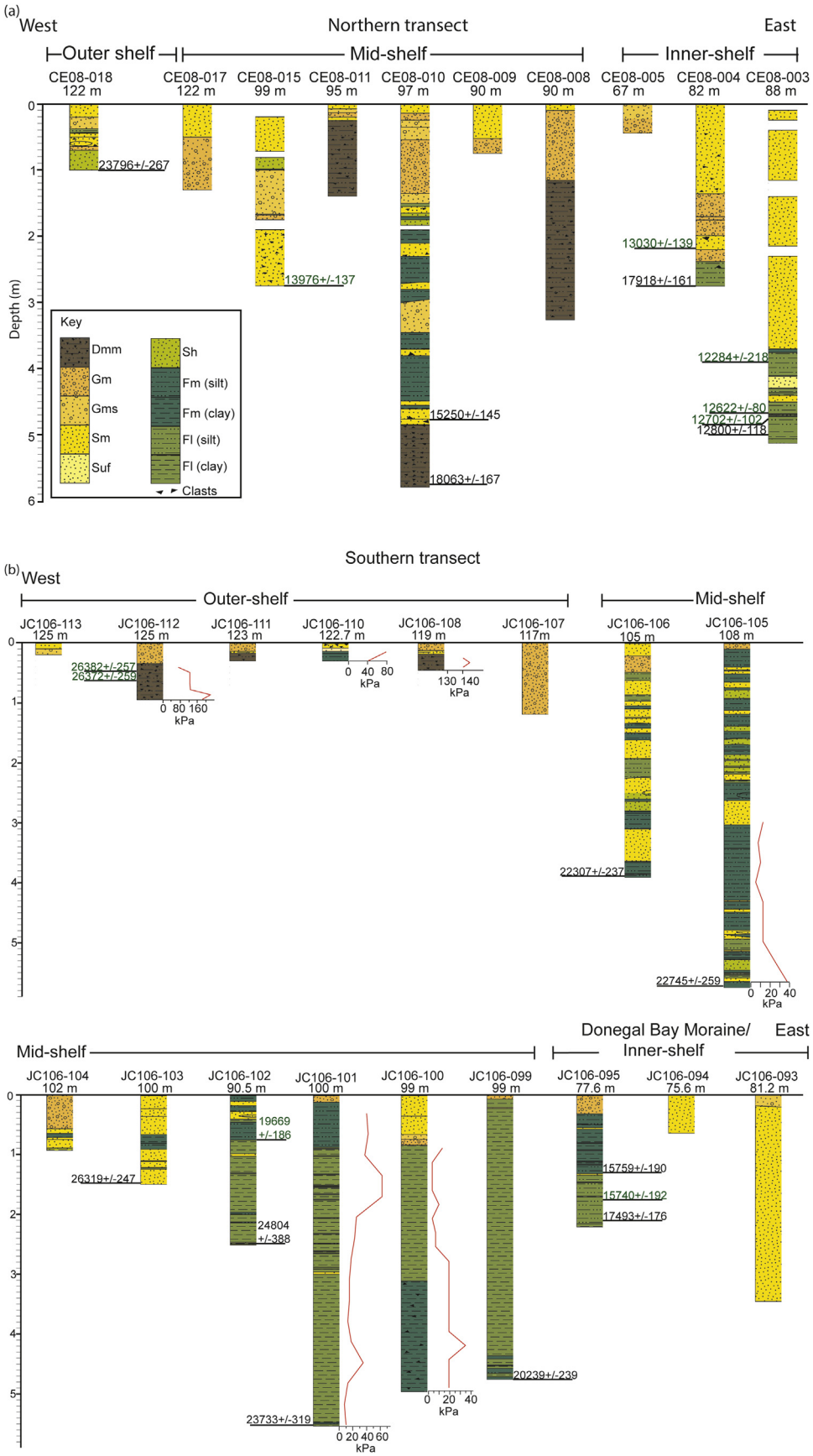

Fig. 6. Core logs presented as a west to east transect from outer shelf to inner shelf. The lithofacies are colour coded. Radiocarbon dates are shown alongside the logs at their stratigraphic depth. Dates in green are from shells, dates in black are from benthic foraminifera. (a) Northern core transect (Celtic Explorer cruise CE08 cores; see Fig. 1). (b) Southern core transect (James Cook cruise JC106 cores; see Fig. 1). Shear strength profiles (in kPa) are also shown in b. (For interpretation of the references to colour in this figure legend, the reader is referred to the Web version of this article.)

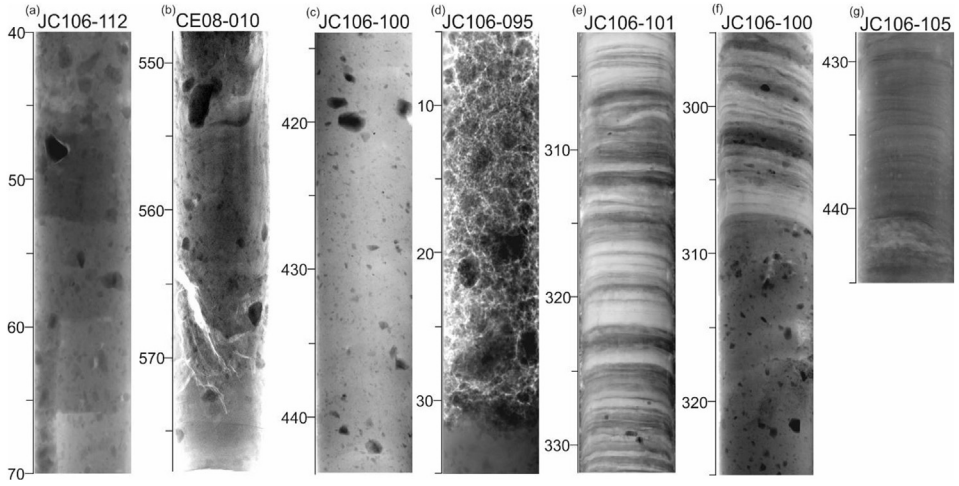

Fig. 7. X-radiographs showing details of lithofacies from the study area. See Fig. 1 for core locations. (a) Facies Dmm. Massive, matrix-supported diamicton from the lower part of core JC106-112 (40–70 cm depth). (b) Facies Dmm-Dml. Massive to diffusely laminated matrix-supported diamicton from the lower part of core CE08-010 (548–578 cm depth). (c) Facies Fmd. Poorly sorted, massive diamictic mud with dispersed clasts. Core JC106-100 (414–445 cm depth). (d) Facies Gm. Clast supported massive gravel. Core JC106-095 (5–35 cm depth). (e) Facies Fl (minor Fld towards bottom of image). Laminated silts and clays. The clays are of higher density and appear as dark bands on the image while silt appears light. Note occasional small pebbles in the lower part of the core. Core JC106-101 (303–332 cm depth). (f) Facies Fmd-Fl. Massive diamictic mud overlain by laminated mud. Note the sharp contact between the two facies and diamictic layers within the upper laminated facies. Core JC106-100 (295–325 cm depth). (g) Facies Sh. Laminated sand. Core JC106-105 (428–445 cm depth).

facies generally range from 0.1 to 1.2 m in thickness. Lower bed contacts are typically sharp and, in some cases, clearly erosive. A common feature of this lithofacies is that it often contains abundant whole or broken shells, and, in cores from the outer shelf, shell fragments constitute a coarse matrix forming a type of 'shell hash'.

4.2.1.8. Lithofacies 8 – matrix-supported, massive gravel (Gms). This facies comprises matrix-supported granule and pebble gravel which is usually massive (e.g., CE08-004, 199-134 cm). The matrix ranges from silty mud to, more commonly, sand, usually coarse. The gravels are often rich in broken and sometimes whole shells forming a 'shell hash'. Individual beds are up to a few tens of centimetres in thickness. Clasts are typically sub-angular to rounded. Lower contacts are sharp and upper contacts range from sharp to gradational.

4.2.2. Lithofacies interpretation and age

The diamicton of Lithofacies 1a is the lowermost stratigraphic unit in cores from the mid- and outer-shelf and is characterised by a massive structure with dispersed clasts in an over-consolidated muddy matrix with fragmented shells. Stratification and grading within the diamicton that might be indicative of subaqueous mass-flow or iceberg-rafting were not observed. Rather its characteristics are more consistent with an origin as a subglacial till with the high shear strengths reflecting loading and compaction by grounded glacier ice (Ó Cofaigh et al., 2007, 2013; J. Evans et al., 2005; D. Evans et al., 2006; Hogan et al., 2016).

The presence of occasional shell fragments within the diamicton indicates that it is formed, at least in part, from the overriding and reworking of pre-existing marine sediment over which the ice sheet advanced (cf. Ó Cofaigh and Evans, 2001; England et al., 2009; Ó Cofaigh et al., 2013). Two AMS radiocarbon dates on individual shell fragments from the diamicton in core JC106-112VC dated 26382 ± 257 cal BP (SUERC-63584) and 26372 ± 259 cal BP (SUERC-63585) (Fig. 6 and Table 2) and provide a maximum age for emplacement of the till and the associated ice sheet advance. They indicate till formation and a grounded ice sheet on the outer shelf after 26.3 ka cal BP.

Although Lithofacies 1b also comprises a stiff, matrix-supported diamicton it differs from Lithofacies 1a in that it is locally transitional to a diffusely laminated diamicton, contains marked variations in clast abundance, dropstones, and it also contains a well preserved glacimarine microfauna (see above and section 5 below). These observations are more consistent with formation of Lithofacies 1b in a glacimarine depositional environment during deglaciation rather than subglacially. The coarse-grained nature of the facies and the high consolidation suggest formation by a combination of the rain-out of iceberg rafted debris and intermittent scouring of the seafloor by grounded iceberg keels (consolidating the sediment)(cf. Dowdeswell et al., 1994; Sacchetti et al., 2012). Radiocarbon dates on two samples of mixed benthic foraminifera from the base of Lithofacies 1b in core CE08-010 and from 6 cm above its upper contact bracket the age of the diamicton and thus glacimarine sedimentation at this core site (mid-shelf). The sample from the core base dated 18063 ± 167 cal BP (SUERC-58324) and the sample from above the diamicton dated 15250 ± 145 cal BP (UCIAMS-133551) (Fig. 6 and Table 2).

Lithofacies 2 comprises fine-grained, soft laminated mud and is common in cores from the mid- and inner-shelf. It corresponds to acoustic Facies B. Lamination is typically horizontal or sub-horizontal and clasts within the muds are small and relatively infrequent. The presence of grading, rhythmicity, sharp laminae bases, and horizontal or sub-horizontal lamination with relatively minor and localised deformation indicates that the laminated muds are a product of meltwater deposition, most likely from the settling of suspended sediment from turbid meltwater plumes issuing from the retreating ice-margin during deglaciation although it is possible that at least some of the lamination is a product of deposition from turbidity currents (Mackiewicz et al., 1984; Hesse et al., 1997; Ashley and Smith, 2000; Ó Cofaigh and Dowdeswell et al., 2001). Clasts within the muds are relatively rare and small implying that iceberg rafting was low and was subsidiary to meltwater deposition (Cowan et al., 1997; Lloyd et al., 2005). Benthic foraminifera indicative of cold, Arctic glacimarine conditions (*E. excavatum f. clavata; Cassidulina reniforme*) are common in Lithofacies 2 and 3 (see section 5 below) indicating that subaqueous sedimentation and ice-sheet retreat occurred in a glacimarine depositional environment (cf. Hald and Korsun, 1997; Lloyd et al., 2005; Jennings

et al., 2006).

Lithofacies 3, massive mud (Fm) is interpreted as a product of rapid meltwater sedimentation in which high sedimentation rates of fine-grained material settling from suspension suppressed the formation of laminations. A similar origin is proposed for the formation of the massive mud with clasts (Fmd) but one in which the rain-out of iceberg-rafted debris played a significant role (Elverhøi et al., 1983; Domack, 1984; McCabe et al., 1986; Dowdeswell et al., 1994).

Radiocarbon dates from the laminated and massive glacimarine mud facies (lithofacies 2 and 3) provide age constraints on the timing of glacimarine sedimentation on the mid-shelf and thus ice sheet retreat. Five dates were obtained from samples of mixed benthic foraminifera from the bases of cores JC106-099VC, JC106-101VC, JC106-102VC, JC106-105VC and JC106-106VC. The oldest date is 24804 ± 388 cal BP (UCIAMS-164437) with the other dates ranging from 23.7–20.2 ka cal BP (UCIAMS-164431, UCIAMS-164438, UCIAMS-164435, UCIAMS-164429) (Fig. 6 and Table 2). Further inshore two samples of mixed benthic foraminifera from laminated glacimarine muds close to the base of core JC106-095VC from the Donegal Bay Moraine and from core CE08-004 from immediately inshore of the moraine dated 17,493 ± 176 cal BP (SUERC-63557) and 17,918 ± 161 cal BP (SUERC-47522) respectively (Fig. 6 and Table 2).

Both lithofacies 2 and 3 infill basins between moraines across the shelf (acoustic Facies B) and, on the mid-shelf, blanket the moraines themselves (Fig. 3). This implies they initially formed time-transgressively in association with successive stillstands of the grounded ice-sheet margin at the moraines. Sedimentation was by a range of glacimarine processes including suspension settling from meltwater plumes, rain out of iceberg-rafted debris (IRD) and dilute sediment gravity flows.

Lithofacies 4 - Laminated or stratified sand facies (Sh) are relatively thin, are characterised by blurred or sharp boundaries, are clast poor and sometimes disturbed. The sands are interpreted as a product of emplacement by discrete sandy gravity flows, probably sandy turbidites. The contorted, disrupted appearance to some beds suggests that they may have undergone slumping and disturbance either pene-contemporaneous with deposition or subsequently (Eyles and Eyles, 2000). The oldest date from this lithofacies is from a sample of mixed benthic foraminifera from the core catcher of core CE08-018 from the outer shelf which dated 23796 ± 267 cal BP (UCIAMS-133552) (Fig. 6 and Table 2).

The normally graded sand of Lithofacies 5 is characterised by sharp lower contacts, concentrations of clasts or shell fragments at the base of beds, and a fining upwards sequence in which sands grade upwards into silts. These features are consistent with an origin as the product of deposition from sandy turbidity currents (Lowe, 1982; Walker, 1992).

Massive sands (Lithofacies 6) with sharp lower contacts and gradational upper contacts with muds are most likely a product of the freezing of dilute sediment gravity flows with the finer grained material settling out of suspension. However, massive sands are also common in the top sections of cores across the shelf (Fig. 6), where they are typically associated with the gravels of Lithofacies 7 (Gm) and 8 (Gms). They contain abundant single and broken shells, often in the form of a 'shell hash' and coarser horizons or bands of pebbles or granules. Lithofacies 6, 7 and 8 therefore comprise an association of variably-sorted, sandy and gravelly facies that are predominantly massive and are the uppermost stratigraphic units in sediment cores from across the shelf. We interpret these sediments as postglacial formed predominantly by the activity of bottom currents on the shelf (cf. Anderson et al., 1984; Howe et al., 2001). Zones of upwards fining sand record either reworking by gradually weakening bottom currents or a marine transgression (Viana et al., 1998). Shell hash, granule and pebbly horizons within massive sands, and clast-supported gravel are likely to be lag deposits.

4.3. Foraminiferal analysis

The aim of the foraminiferal analysis was to provide additional information on the depositional environment(s) across the continental shelf through time to combine with the lithofacies and acoustic facies analysis. To achieve this six cores were selected from the outer to inner shelf: CE08-018 from the outer shelf; CE08-010, JC106-100 and JC106-102 from the mid-shelf; and JC106-095 and CE08-003 from the Donegal Bay Moraine and inner shelf respectively. Sample selection was concentrated in particular on the lower sections of the cores with the aim of understanding depositional environments during deglaciation. Other sections of the cores were also sampled to aid in the interpretation of depositional environments. Acoustically, most of the sediments sampled were from acoustic Facies B.

Foraminifera were counted from a total of 63 samples and a total of 48 benthic foraminiferal species were identified (45 calcareous and 3 agglutinated species). Planktonic foraminifera were also counted, but were not identified to species level and have not been included in the percentage calculation. The following sections provide a brief description and interpretation of the foraminiferal assemblage data (see SOI for a full species list and detailed count data).

4.3.1. CE08-018 (outer-shelf)

Foraminifera were counted from four samples from the base of the core (100 cm) up to 62 cm (Fig. 8). The samples were from Lithofacies 4 (Sh). The assemblage is dominated by *Cibicides lobatulus* (24–53%) and *Elphidium excavatum f. clavata* (16–40%) with *Cassidulina reniforme* (4–22%) also common (Fig. 8). There are minor occurrences of *Cassidulina laevigata* (up to 5%) and *Quinqueloculina seminulum* (increasing to 12%).

Interpretation: The dominance of *C. lobatulus* indicates relatively coarse sediment grain size associated with strong bottom water currents (Jennings et al., 2006; Hald and Korsun, 1997) while the co-dominance of *E. excavatum f. clavata* and with *C. reniforme* also common indicates a glacimarine environment. These latter two species are typically found in modern Arctic fjord and shelf environments with *E. excavatum f. clavata* in particular being common in proximal glacimarine environments while *C. reniforme* tends to dominate in more distal glacimarine and cold polar water dominated environments (e.g. Hald and Korsun, 1997; Korsun and Hald, 1998). Indeed *C. lobatulus*, while not typically a glacimarine species, is common in Arctic fjord and shallow shelf environments associated with strong meltwater fluxes from tidewater glacier margins (e.g. Jennings et al., 2006). A mixed benthic foraminifera sample from the core catcher dated 23,796 ± 237 cal BP (UCIAMS-133552) (Fig. 6, Table 2).

4.3.2. CE08-010 (mid-shelf)

Foraminifera were counted at 16 cm intervals from the base of the core (578 cm) up to a depth of 144 cm, and thus from a range of lithofacies (lithofacies 1, 2, 3, 5, 6 and 7) (Fig. 8). The assemblage through this core is dominated by three species, *Elphidium excavatum f. clavata*, *Cassidulina reniforme* and *Cibicides lobatulus* (Fig. 8). The core can be divided into 5 foraminiferal assemblage zones, FAZ 1 to FAZ 5. The lower zone, FAZ 1 (samples from 578 to 528 cm), is dominated by *E. excavatum f. clavata* (35–70%) with *C. reniforme* also abundant (20–33%). Absolute abundance in this section is rather low, with total foraminifera counted generally below 100 specimens, the abundance of planktic foraminifera is

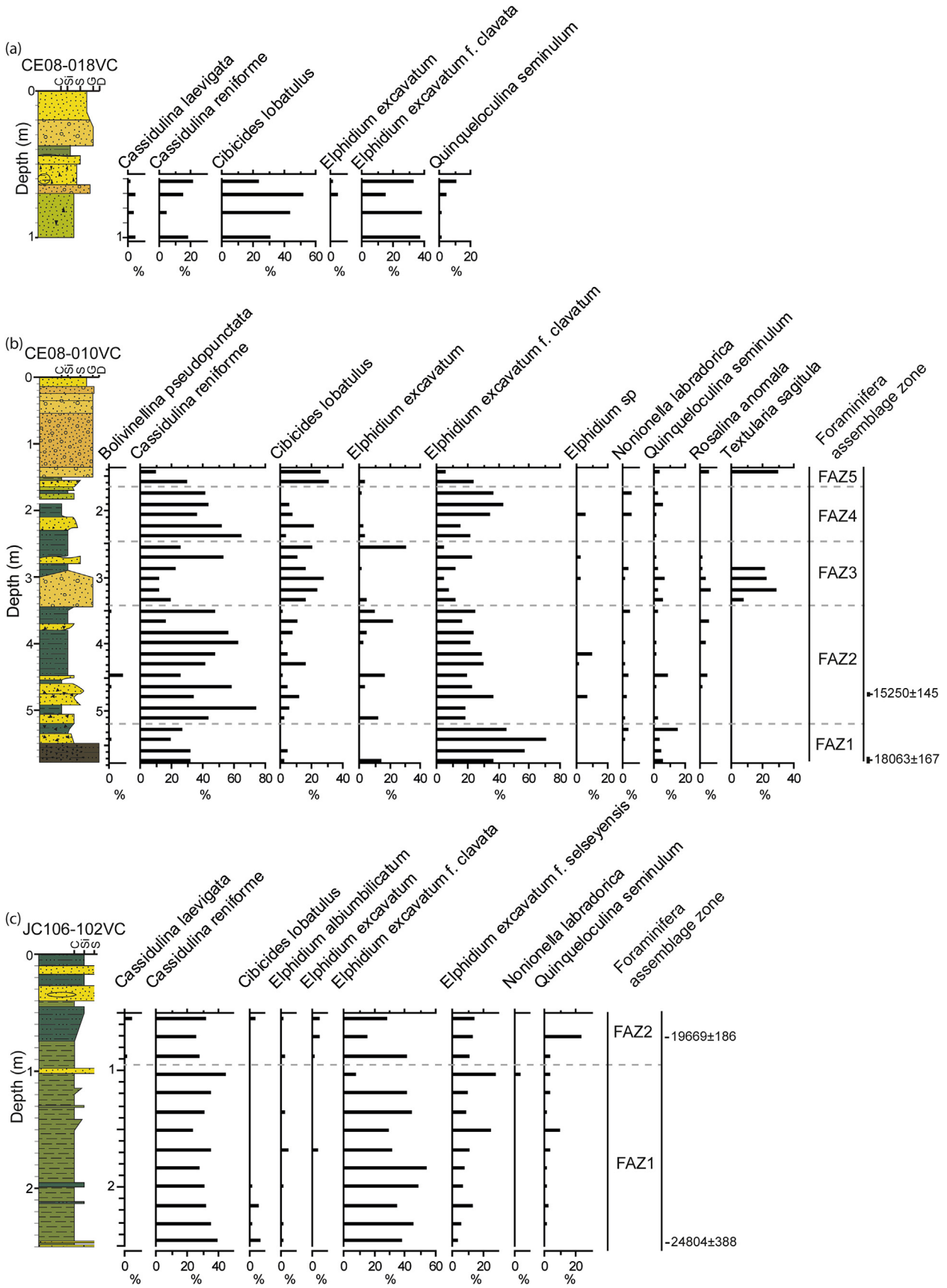

Fig. 8. Foraminiferal assemblage data from cores along a transect from outer-to inner-shelf: (a) CE08-018 (outer shelf); (b) CE08-010 (mid-shelf); (c) JC106-102VC (mid-shelf); (d) JC106-100 (mid-shelf); JC106-095VC (Donegal Bay Moraine); and (f) CE08-003 (inner-shelf).

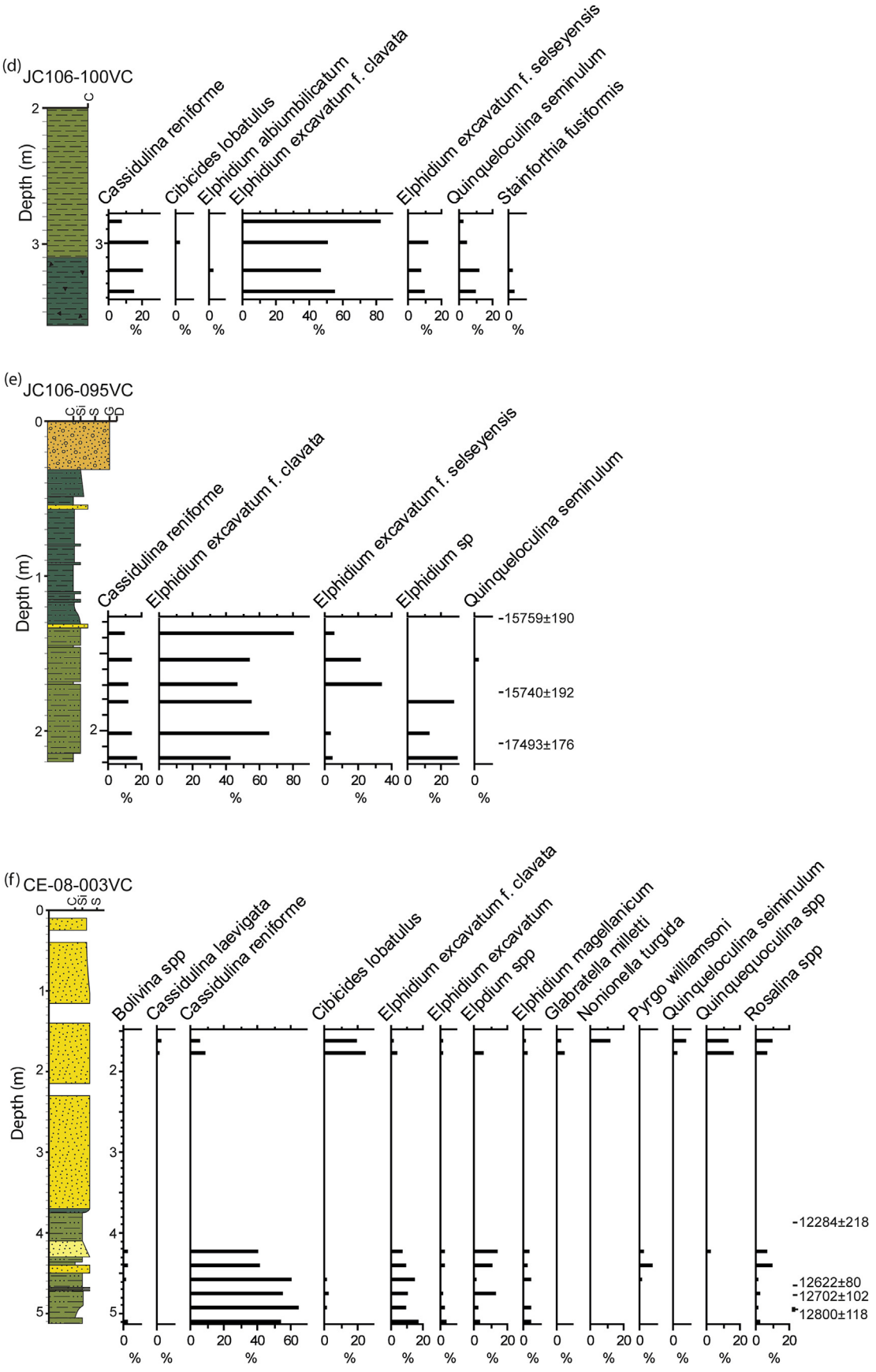

Fig. 8. (*continued*).

also low. FAZ 2 (samples from 512 to 352 cm) is dominated by *C. reniforme* (16–75%) with *E. excavatum f. clavata* still abundant (20–40%) and *Cibicides lobatulus* becoming more common (5–15%). Absolute abundance and the number of planktic foraminifera increase in this zone. There is a significant change with the transition to FAZ 3 (samples from 336 to 256 cm) with *C. lobatulus* becoming dominant (17–28%) and a decrease in abundance of *C. reniforme* (12–23%) and *E. excavatum f. clavata* (5–13%). FAZ 4 (samples from 240 to 176 cm) is characterised by a gradual decrease in abundance of *C. lobatulus* (17% decreasing to 0%) as *C. reniforme* (26–63%) and *E. excavatum f. clavata* (5–45%) both increase to co-dominate. This trend is reversed in FAZ 5 as *C. lobatulus* increases to dominate the assemblage again while *C. reniforme* and *E. excavatum f. clavata* both decrease.

Interpretation: The benthic foraminiferal assemblage in FAZ 1, dominated by *E. excavatum f. clavata* and *C. reniforme*, is indicative of a glacimarine environment. This is also supported by the relatively low absolute abundance indicative of the relatively harsh conditions in a glacimarine setting. FAZ 1 is characterised by a matrix-supported diamicton that ranges from massive to diffusely laminated at the base of the core (see section 4 above) and a radiocarbon date on benthic foraminifera from the base returned an age of 18,063 ± 167 cal BP (SUERC-58324) (Fig. 6 and Table 2). The increase in abundance of *C. reniforme*, but still with a relatively high proportion of *E. excavatum f. clavata* through FAZ 2 indicates more distal glacimarine conditions (allowing a greater absolute abundance of foraminifera to develop). Sedimentologically this change in environments is associated initially with the upper part of Lithofacies 1b (diamicton) which fines upwards through massive sands (Sm) into laminated and massive mud (Fld, Fm, Fmd). A sample of mixed benthic foraminifera from massive sand 6 cm above the contact with the diamicton dated 15,250 ± 145 cal BP (UCIAMS-133551) (Fig. 6 and Table 2). The major shift into FAZ 3 indicates increasing distance from a glacimarine environment, but still relatively cold polar waters, with an increase in species other than glacimarine indicators, principally *C. lobatulus* and also the appearance of *C. laevigata*. The dominance of *C. lobatulus* is associated with an increase in sediment grain size indicative of stronger bottom water currents. Supporting this interpretation, the lithofacies within this zone are dominated by matrix-supported gravels (Gms) which may, at least in part, represent a lag deposit. Lower energy conditions then return during the deposition of FAZ 4 with continuing distal glacimarine/cold polar water conditions (*C. reniforme* dominant). This transition is also marked by a return to finer grained sediments, predominantly massive silts and clays (Fm), and massive sand (Sm) often associated with higher abundance of *C. lobatulus*. Higher energy conditions then return during the deposition of FAZ 5 (a mixture of massive sands and gravels, (lithofacies Sm and Gms) with an assemblage dominated by *C. lobatulus*.

4.3.3. JC106-102 (mid-shelf)

Foraminifera were counted at 16 cm intervals from 248 cm (near the base of the core) up to 56 cm (Fig. 8). The samples were from the laminated and massive mud of Lithofacies 2 and 3. The assemblage shows limited variability, but can be divided into two zones (Fig. 8). FAZ 1 from 248 to 88 cm is associated with a thick sequence of Lithofacies 2 (laminated mud) and is dominated by *E. excavatum f. clavata* (30–54%) and *C. reniforme* (24–46%), with *Elphidium excavatum f. selseyensis* also common. The transition to FAZ 2 is characterised by a slight increase in other species such as *C. lobatulus, C. laevigata* and *Elphidium excavatum*, though while there is a reduction in *Elphidium excavatum f. clavata* in particular and also in *C. reniforme*, these two species still dominate the assemblage. FAZ 2 is associated with Lithofacies 3 (massive mud; Fm, Fmd).

Interpretation: The dominance of *E. excavatum f. clavata* and *C. reniforme* through this core indicates a glacimarine environment, becoming progressively more distal through FAZ 1 and into FAZ 2 in particular as the abundance of *E. excavatum f. clavata* gradually decreases and other species, such as *E. excavatum f. selseyensis* (a cold water rather than glacimarine indicator) and *C. laevigata*, increase slightly. This interpretation is consistent with the lithofacies through this section which comprise laminated muds overlain by massive muds and with a slight increase in silt content through FAZ 2. A sample of mixed benthic foraminifera from the base of the core dated 24,804 ± 388 cal BP (UCIAMS-164437) (Fig. 6 and Table 2).

4.3.4. JC106-100 (mid-shelf)

Foraminifera were counted from four samples taken from the lower section of this core, 336 to 284 cm (Fig. 8). The samples extend across a lithofacies transition from massive diamictic mud (Lithofacies 3) to laminated mud (Lithofacies 2) at 310 cm depth. The assemblage is dominated by *E. excavatum f. clavata* (50–80%) with *C. reniforme* also abundant (10–20%) and *E. excavatum f. selseyensis* and *Quinquelocaulina seminulum* also common (5–10%).

Interpretation: The dominance of *E. excavatum f. clavata* with *C. reniforme* also common indicates a glacimarine environment through this section of massive diamictic mud and then laminated silts and clays (lithofacies Fmd to Fl).

4.3.5. JC106-095 (Donegal Bay Moraine)

Foraminifera were analysed from the lower section of this core, six samples from 218 to 138 cm (Fig. 8). The samples were collected from Lithofacies 3 (laminated mud). The assemblage is dominated by *E. excavatum f. clavata* (40–80%) with other species of *Elphidium* also dominant and *C. reniforme* common (15–20%) (Fig. 8).

Interpretation: The abundance of *E. excavatum f. clavata* indicates a glacimarine environment, likely to be relatively proximal due to the dominance of this species. *C. reniforme*, more of a distal glacimarine to cold polar water indicator and *E. excavatum f. selseyensis*, associated with cold waters, are also common. The sedimentology of this section of the core is dominated by laminated silts and clays (Lithofacies 2, Fl). A sample of mixed benthic foraminifera from laminated muds at 209 cm and a shell fragment from 175.5 cm depth dated 17,493 ± 176 cal BP (SUERC-63557) and 15,740 ± 192 cal BP (SUERC-58403) respectively (Fig. 6 and Table 2).

4.3.6. CE08-003 (inner-shelf)

Foraminifera were counted from two sections in this core, a lower set of six samples from 510 to 425 cm, primarily from laminated mud (Lithofacies 2) with minor upwards fining sand (Lithofacies 5), and then an additional two samples from a shallower section, 180 to 162 cm from massive sand (Lithofacies 6) (Fig. 8). The core can be split into three foraminiferal assemblage zones, FAZ 1 to FAZ 3 (Fig. 8). FAZ 1 from 510 to 459 cm is dominated by *C. reniforme* (50–60%) with *E. excavatum f. clavata* also common (15–20%) and other species of *Elphidium* also present. There is a subtle change in assemblage from 442 to 425 cm (FAZ 2). There is a slight decrease in abundance of *C. reniforme*, though this species still dominates (40%), there is also a slight decrease in abundance of *E. excavatum f. clavata* (<10%) and several other species become more common, such as *Pygo williamsoni* and *Rosalina spp*. The upper section of the core (FAZ 3 from 180 to 162 cm) has a significantly different assemblage with a wider range of species abundant and no clear dominant species. *Cibicides lobatulus* and *Quinqueloculina spp.* are most abundant (20–30%) and *Glabratella milletti, C. laevigata, Nonionella turgida* and *Miliolinella* also present in low abundances. Radiocarbon dates on four samples from the laminated muds provide a core chronology. A mixed benthic foraminifera sample from 493 to 499 cm dated 12,800 ± 118 cal BP (UCIAMS-133550);

two single valves of *Macoma calcarea* from 477 cm to 466 cm dated 12,702 ± 112 cal BP (SUERC-47516) and 12,622 ± 80 cal BP (SUERC-47515); and a shell fragment from 387 cm depth dated 12,284 ± 218 cal BP (SUERC-47514) (Fig. 6 and Table 2).

Interpretation: The abundance of *C. reniforme* in FAZ 1 indicates cold polar water conditions, potentially distal glacimarine, particularly with the presence of *E. excavatum f. clavata*. The abundance of glacimarine species decreases in FAZ 2 as abundances of other typical North Atlantic boreal species increase (for example *P. williamsoni* and *Rosalina spp.*). The upper section of the core, FAZ 3, is characterised by a further reduction in glacimarine species (<10%) as a more diverse range of typical North Atlantic boreal species dominate the assemblage. The relatively high abundance of *C. lobatulus* (20%) suggests higher bottom water current speeds with an associated increase in sand content.

5. Discussion

5.1. Ice sheet extent on the continental shelf northwest of Ireland at the LGM

On the basis of six terrestrial ^{36}Cl surface exposure dates of 36.5 ± 3.6 ka to 25.1 ± 1.1 ka obtained from ice-moulded bedrock or erratic boulders at widely separated sites Bowen et al. (2002) proposed that the last ice sheet in Ireland reached its maximum extent before ~37.5 ka (during Marine Isotope Stage 3), and was more restricted during the subsequent lLGM. This view was supported by McCabe et al. (2007a) on the basis of a set of fifteen radiocarbon dates from stratigraphic sequences at Glenulra on the south side of Donegal Bay. Eleven dates were on reworked single *Arctica islandica* shells from either till or deglacial outwash and ranged from ~43.3 to ~26.1 ka cal BP. The final four dates were from 27.8 to 25.3 cal ka BP obtained from *Elphidium clavatum* tests interpreted as in-situ by McCabe et al. from raised marine muds. They inferred that high relative sea levels, implying marked isostatic depression and thus the proximity of a thick ice sheet, had persisted over a period of ~20 ka prior to the gLGM and that the ice sheet underwent a rapid advance-retreat on the continental shelf about 28 ka cal BP and thus immediately prior to the lLGM, although offshore evidence from the shelf was not presented (see Ballantyne and Ó Cofaigh 2016).

By contrast, Greenwood and Clark (2009) and Clark et al. (2012) argued on the basis of glacial geomorphological mapping that a major ice stream flowed onto the shelf through Donegal Bay at the lLGM. This supported the results of an earlier study by Ballantyne et al. (2007) based on cosmogenic surface exposure dating and trimline mapping which proposed a lLGM ice sheet that extended at least 20 km across the shelf from the present coastline. Ó Cofaigh et al. (2012) mapped streamlined subglacial bedforms on the inner continental shelf and arcuate moraines that extend across the shelf from the mouth of Donegal Bay to the shelf edge. They interpreted the moraines as recording the former presence of a grounded, shelf-edge terminating ice sheet that then underwent lobate, episodic retreat back across the shelf and into Donegal Bay. This is consistent with glacial geomorphological mapping by Dunlop et al. (2010) from the Malin Sea immediately to the north, which indicated extensive shelf edge glaciation with convergent ice flows from western Scotland and northwest Ireland reaching the shelf edge at the lLGM. Ó Cofaigh et al. (2012) suggested an lLGM age for the shelf-edge advance offshore Donegal Bay based on comparison to the timing of BIIS IRD fluxes onto the Barra Fan which implied that maximum ice sheet growth was attained by 24 cal ka BP and deglaciation occurred at 23 cal ka BP (Scourse et al., 2009). However, the moraines were not dated directly and thus the timing of ice sheet advance and retreat across the Atlantic shelf northwest of Ireland remained poorly constrained until the present study.

Working further to the south, offshore of Galway Bay, Peters et al. (2015, 2016) presented marine geophysical and geological evidence supported by radiocarbon dating which indicated that the last BIIS extended across the shelf west of Ireland and onto the Porcupine Bank, with retreat underway by 21.8 cal ka BP. Extensive grounded ice on the shelf is also supported by the recent study of Callard et al. (2018) from the Malin Sea. These authors propose advance of the Barra Fan Ice Stream to the shelf edge west of Scotland at the lLGM with retreat underway by 25.9 cal ka BP and the majority of the shelf ice free by 23.2 cal ka BP.

Cores JC106-108VC, JC106-111VC and JC106-112VC from the outer shelf offshore Donegal Bay recovered stiff, matrix-supported diamictons (see above). The characteristics of these diamictons are consistent with their formation as subglacial tills associated with a grounded ice sheet. Two AMS radiocarbon dates on reworked shells from JC106-112VC provide a maximum age for till formation and thus the advance of ice onto the outer shelf (see above). They indicate this occurred after 26.3 ka cal BP (Fig. 9). This was a little later than previous interpretations of the timing of the lLGM at 27 ka (C. Clark et al., 2012), but is consistent with IRD records from the Barra Fan which indicate shelf-edge glaciation occurred after 27 ka (Scourse et al., 2009).

Retreat of the ice sheet from the outer shelf is constrained by several dates from laminated sand and mud facies that record glacimarine conditions during deglaciation in cores from the outer and mid-shelf. A date of 23,796 ± 267 cal BP (UCIAMS-133552) from mixed benthic foraminifera in core CE08-018 dates retreat from the outer shelf but older dates from the mid-shelf of 24,804 ± 388 cal BP (UCIAMS-164437) from glacimarine muds in JC106-102VC and 26,319 ± 247 cal BP (SUERC-63558) from massive sands at the base of JC106-103VC indicates that the ice sheet retreat from the outer shelf was actually underway before this time. The date of 26,319 ± 247 cal BP (SUERC-63558) is within the 2 sigma error range of the dates from till in core JC106-112VC. This either implies a very short-lived rapid advance/retreat on the outer shelf or, perhaps more likely, that the date of 26,319 ± 247 cal BP is actually a maximum constraint on retreat. Either way the dates on reworked shells from tills and on benthic foraminifera from glacimarine deposits constrain the most recent episode of ice occupancy on the outer shelf to between 26.3 and 24.8 cal ka BP and thus during the gLGM when eustatic sea level was at a minimum (P. Clark et al., 2009; Lambeck et al., 2014). This implies the existence of ice free conditions and crustal depression immediately prior to that advance, at least on the outer shelf.

The new radiocarbon dates from till and deglacial sediments that we present in this study provide directly dated evidence for an extensive grounded ice sheet offshore of northwest Ireland at the gLGM. It is consistent with earlier work which proposed a similar reconstruction on geomorphological grounds (Dunlop et al., 2010; Ó Cofaigh et al., 2012), and a recent study from the Malin Sea Shelf which inferred a shelf edge advance of the Barra Fan Ice Stream after 26.7 cal ka BP (Callard et al., 2018). Collectively we suggest that this implies a shelf-edge terminating BIIS along the continental margin offshore of northwest Ireland and western Scotland at the lLGM. This counters earlier proposals (Bowen et al., 2002; McCabe et al., 2007a), which argued for a restricted LGM advance onto the shelf in this region. Given the weight of geomorphological, sedimentological and chronological evidence for a grounded ice sheet emanating from Donegal Bay and extending to the shelf edge at the LGM the four Glenulra dates on benthic foraminfera (McCabe et al., 2007b) are inferred to be anomalous (Ballantyne and Ó Cofaigh, 2016). As proposed by Ballantyne and Ó Cofaigh (2016) they could be explained by preservation beneath LGM ice, possibly in permafrost, due to their protected position in a valley orthogonal to

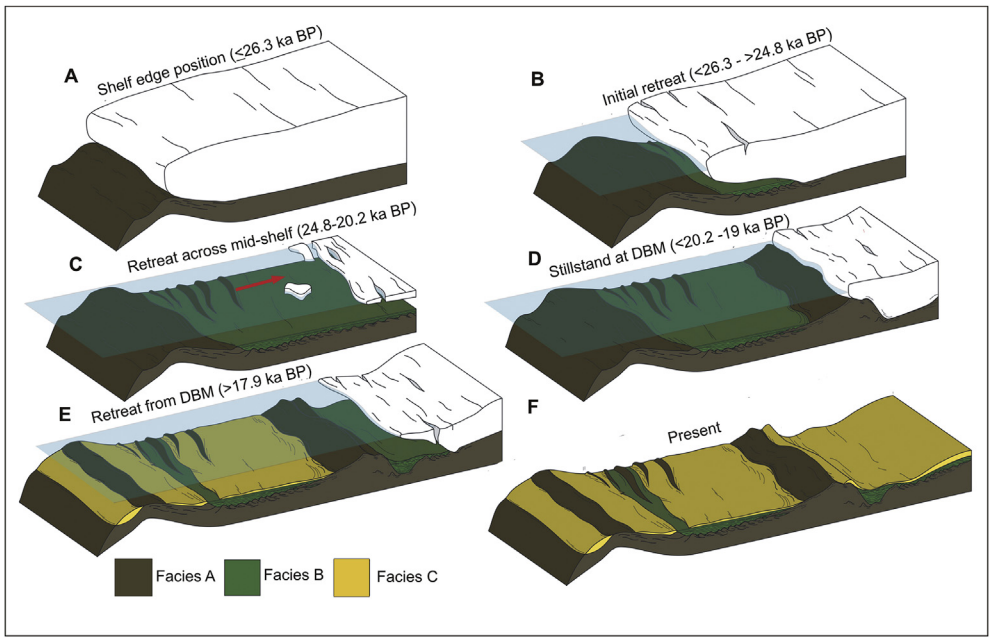

Fig. 9. Reconstruction of glacial and deglacial history on the continental shelf northwest of Ireland. (A) Shelf-edge ice sheet at LGM (≤26.3 ka BP). (B) Initial ice sheet retreat from shelf edge (<26.3->24.8 ka BP). (C) Ice sheet retreat across the mid-shelf (24.8–20.2 ka BP). (D) Ice sheet marginal stillstand at the Donegal Bay Moraine ('DBM') (<20.3->17.9 ka BP). (E) Retreat from the Donegal Bay Moraine ('DBM') (≥17.9 ka BP). (F) Present day. Acoustic Facies A-C are also indicated.

the direction of ice sheet flow, or alternatively they are reworked and thus provide only maximum ages for the timing of ice sheet retreat.

5.2. Glacimarine conditions during deglaciation

Our sedimentological and foraminiferal data demonstrate that retreat of the last ice sheet across the Atlantic shelf northwest of Ireland took place in a glacimarine environment (Fig. 9). This interpretation is supported by laminated and massive muds with dropstones (lithofacies 2 and 3 above) that contain a foraminiferal assemblage with abundant *E. excavatum f. clavata* and *C. reniforme*. These species are common in modern glacier-influenced, Arctic fjord and shelf environments which are characterised by low salinity and cold temperatures (Hald and Korsun, 1997; Korsun and Hald, 1998; Lloyd, 2006). Present day water depths in the study area are deepest at the shelf edge (125 m) but then decrease to less than 80 m at the mouth of Donegal Bay, where the Donegal Bay Moraine is located. The cores containing glacimarine sediments generally were recovered in water depths of ca. 75–105 m. Given a global eustatic lowstand of −134 m at the gLGM (Lambeck et al., 2014) this indicates isostatic depression of at least 25–55 m on the shelf. However, the presence of marine muds up to 10 m asl with in-situ glacimarine macro- and microfauna dated to the last deglaciation from the south side of Donegal Bay at Belderg and Fiddauntawnanoneen imply that crustal depression was probably at least 145 m (McCabe et al., 1986, 2005, 2007a). It is possible that this GIA-induced sea-level rise was augmented by any rise associated with the H2 event (24 ka; Hemming, 2004; Scourse et al., 2009). However, estimates of sea-level rise associated with the Heinrich events are 3–15 m (Hemming, 2004), and the H2 event is not visible in the eustatic sea-level curve of Lambeck et al. (2014). Thus the relative sea level rise recorded by the glacimarine sediments across the shelf and onshore in southern Donegal Bay must have been predominantly a consequence of local glacioisostatic depression. This was likely a cummulative effect involving crustal depression during both ice sheet build-up and glacial maximum.

The seafloor bathymetric data on the sediment ridges across the shelf shows they are sharp-crested, nested and lobate. They differ in morphology from grounding-zone wedges, often described from polar continental margins, which tend to be asymmetric with a gentler stoss- and steeper lee-slopes, have a distinct wedge-like geometry, may have internal bedding or 'foresets' and may be over-printed by subglacial lineations and/or iceberg scours (e.g., Ó Cofaigh et al., 2005; Evans et al., 2005; Dowdeswell and Fugelli, 2012; Batchelor and Dowdeswell, 2015; Livingstone et al., 2016). This suggests that the BIIS retreated across the northwest shelf as a grounded tidewater margin rather than as an ice-shelf. Further indirect support for this interpretation is provided by the thick sequences of laminated and massive muds with dropstones and abundant foraminifera in the sediment cores. These record deposition by suspension-settling from meltwater plumes combined with rain out of ice-rafted debris as well as sandy mass flows (cf. Mackiewicz et al., 1984; Pfirman and Solheim, 1989; Powell and Domack, 1995). Ice-shelf facies in contrast tend to be characterised by coarse-grained, sometimes rubbly, diamictons, pelletised mud facies and massive clast-free muds overlain by diatomaceous open marine muds with IRD (cf. Domack and Harris, 1998; Powell et al., 1996; Domack et al., 1999; Evans et al., 2005; Kilfeather et al., 2011).

5.3. Timing and drivers of ice sheet retreat

Initial retreat from the outer shelf was complete at or before 24.8 cal ka BP by which time the ice sheet was depositing deglacial glacimarine facies on the mid-shelf (Fig. 9). Dates from cores that bottomed out in glacimarine sediments on the mid-shelf gave ages of 23.7–22.3 ka cal BP (Fig. 5). Although these are interpreted as minimum ages on retreat across the mid-shelf (i.e., retreat occurred earlier than these dates), in conjunction with the earlier dates of 26.3–24.8 ka cal BP they provide a consistent chronology that indicates ice sheet recession across the shelf occurred early during the last deglaciation. This is consistent with work from further north in the Malin Sea where Callard et al. (2018) demonstrate that

retreat from the shelf edge was underway by 25.9 cal ka BP. However, it is ca. 3–4 ka earlier than previous estimates of retreat further to the south on the western shelf (Peters et al., 2016) and is also earlier than the date of 23 ka for deglaciation inferred from deep sea IRD records of the BIIS (Scourse et al., 2009).

The Donegal Bay Moraine marks a major ice-marginal position on the inner shelf (Figs. 2 and 9). Acoustic profiles from across the moraine show that it is comprised of two ridges (Fig. 5). The acoustic profiles also imaged deformed acoustic Facies B (stratified glacimarine deposits) both behind and within the moraine (Fig. 5). This suggests that formation of the moraine may relate to a readvance or oscillation of the ice sheet margin during deglaciation. The age of the moraine is constrained by radiocarbon dates on glacimarine muds in three cores from either side and from the top of the moraine. Glacimarine sediments from the base of core JC106-99VC from west of the moraine dated 20,239 ± 239 cal BP (UCIAMS-164429) and in core CE08-004 east of the moraine dated 17,918 ± 161 cal BP (SUERC-47522). A further sample from core JC106-095VC collected from between the two moraine crests dated 17,493 ± 176 cal BP (SUERC-63557) (Fig. 6 and Table 2). The age of the moraine is thus bracketed to between 20.2 and 17.9 cal ka BP. Thus, contrary to some previous interpretations (J. Clark et al., 2009), the moraine pre-dates the Killard Stadial readvance (~17.3–16.5 ka; McCabe et al., 2007b; J. Clark et al., 2009) and was formed earlier, during deglaciation of the shelf at ca. 20–19 ka cal BP. The position of the moraine is consistent with an interpretation of the ice sheet margin slowing as it retreated from the wide continental shelf back into the narrower confines of Donegal Bay (cf. Jamieson et al., 2012).

Our interpretation of episodic ice sheet retreat across the Atlantic shelf northwest of Ireland is supported regionally by several studies from offshore western Ireland and Scotland. Peters et al. (2016) document a large, arcuate, glacigenic depocentre on the mid-shelf offshore Galway Bay that they interpret as a grounding-zone wedge marking a major stillstand during deglaciation. They term this feature the 'Galway Lobe Grounding Zone Wedge' (GLGZW). As with the Donegal Bay Moraine (see above), Peters et al. (2016) infer that the GLGZW records periods of local ice re-coupling or readvance based on the presence of glacitectonised glacimarine sediments on its flanks. However, it differs from the Donegal Bay Moraine in an apparent absence of topographic control on its formation. Further to the north, in the Malin Sea, Callard et al. (2018) have presented marine geophysical evidence for grounding zone wedges, and thus episodic retreat, dating to the last deglaciation of the outer-to mid-shelf. Topography appears to have exerted a strong control on retreat dynamics once the ice sheet reached the fjords and islands of western Scotland which acted as pinning points (Small et al., 2017).

The ice sheet underwent ~81 km of retreat from the shelf edge to the Donegal Bay Moraine which formed ca. 20–19 ka BP. Dates of 26.3 ka from reworked shells in till from the outer shelf provide a maximum age for the timing of retreat and a date of 24.8 ka from glacimarine sediments on the mid-shelf provides a minimum age for retreat from the outer shelf. These dates allow an envelope of retreat rates to be estimated. If these are averaged across the outer shelf to the Donegal Bay Moraine they range from 11.25 m/yr to 14 m/yr. It is, however, perhaps more instructive to break this down further into retreat from the shelf edge to the mid-shelf (core JC106-102VC with retreat dated at 24.8 ka BP) and then retreat from JC106-102VC to the Donegal Bay Moraine over distances of 50 km and 32 km respectively. This gives a minimum retreat rate of 35.7 m/yr from the shelf edge to the mid-shelf with the caveat that this retreat must actually have been faster as the 26.3 ka date constraining pull-back from the shelf edge is a maximum date for retreat. Ice sheet retreat then slowed to 5.5 m/yr from core site JC106-102VC to the Donegal Bay Moraine. While retreat across the outer shelf was faster when compared to that from the mid-shelf to the Donegal Bay Moraine, overall these retreat rates are slow and consistent with the geomorphological evidence which points to episodic retreat characterised by numerous still-stands. By way of comparison they are an order of magnitude less than retreat rates recorded for contemporary ice streams in West Antarctica (e.g., 120–450 m/yr; Conway et al., 1999; Thomas et al., 2011) and the largest ice stream of the BIIS the Irish Sea Ice Stream (100–550 m/yr; Chiverrell et al., 2013). These relatively slow retreat rates offshore NW Ireland are consistent with the predominantly normal bed slope across the shelf and lack of major overdeepenings (cf. Briner et al., 2009; Stokes et al., 2014).

Our radiocarbon chronology indicates that the timing of initial BIIS retreat from the Atlantic shelf offshore of NW Ireland occurred relatively early during the gLGM (Clark et al., 2009), thereby implying that atmospheric warming is unlikely to have been the main driver of initial retreat. Furthermore, the foraminiferal assemblages within the cores show no evidence for the advection of warm ocean waters during initial deglaciation across the shelf. Rather they are dominated by glacimarine and cold-water indicator species. This, and the presence of glacimarine sediments along the adjoining coastline of north Mayo (see above), argues against ocean warming as a trigger for ice sheet retreat from the shelf and indicates high relative sea level during deglaciation. It is notable that extensive zones of well-developed iceberg ploughmarks occur immediately offshore of the outermost moraines on the shelf (Benetti et al., 2010; Ó Cofaigh et al., 2012). Initial retreat from the shelf edge therefore appears to have been linked to a major episode of ice-sheet break-up and iceberg calving (cf. Bradwell et al., 2008; Small et al., 2017). It is likely that retreat was triggered by relative sea-level rise causing a buoyancy threshold to be crossed and destabilisation of grounded ice at the shelf edge. The early timing of initial retreat (<26.3->24.8 cal ka BP) coincides with the gLGM eustatic sea level lowstand (Lambeck et al. (2014). Hence the high relative sea level must have been predominantly a function of glacioisostatic depression related to the presence of the BIIS.

The concept of high relative sea level due to glacioisostatic depression has long been known (e.g., Walcott, 1970; Andrews, 1970), as has the importance of this for triggering the retreat of marine-based ice sheet sectors (e.g., Andrews, 1987; Hughes, 1987). More recently, modelling has also drawn attention to the important effects of glacioisostatic adjustment in modulating ice age cycles (Abe-Ouchi et al., 2013) and possibly Heinrich events (Bassis et al., 2017). In the case of the BIIS, deglaciation of the Irish Sea Basin was inferred by some workers (Eyles and McCabe, 1989) to have been triggered by rising relative sea level as the basin underwent glacioisostatic subsidence (although aspects of this interpretation have proved controversial; cf. McCarroll, 2001). In their assessment of the timing of the gLGM and the associated controls on ice sheet growth and decay, Clark et al. (2009) argued that many of the northern hemisphere ice sheets, including the BIIS, began to retreat from their maxima at 19–20 ka and that this was triggered by northern insolation. The much earlier deglaciation of the BIIS from the continental shelf offshore of NW Ireland that we document here (cf. Callard et al., 2018) occurred in the absence of external forcing such as atmospheric or ocean warming and was likely driven by glacioisostatic depression and high relative sea level. This demonstrates that marine-based sectors and margins of large ice sheets can trigger their own demise internally through glacioisostatic adjustment and it underscores the importance of including glacioisostasy and relative sea level changes at a high enough spatial and temporal resolution in numerical ice sheet models to ensure that they capture the full range of processes of marine-ice sheet dynamics.

6. Conclusions

- On the Atlantic shelf northwest of Ireland, arcuate moraines imaged in multibeam swath bathymetric and sub-bottom profiler data on the outer shelf and subglacial tills in sediment cores record the former extension of a grounded BIIS to the shelf edge. Radiocarbon dates on reworked shells indicate till formation and ice sheet advance occurred after 26.3 ka cal BP and thus during the gLGM.
- Nested moraines record the subsequent episodic retreat of the ice sheet across the shelf. Acoustically stratified facies formed during deglaciation and cores from these facies recovered laminated and massive muds containing glacimarine foraminiferal assemblages. These landforms and sediments were deposited by a retreating grounded (tidewater) ice sheet margin.
- Radiocarbon dates indicate that the ice sheet had retreated to the mid-shelf by > 24.8 cal ka BP and so initial pull-back from the shelf edge occurred in the interval <26.3->24.8 cal ka BP. A prominent moraine at the mouth of Donegal Bay the 'Donegal Bay Moraine', records a major stillstand and/or readvance during deglaciation, and formed at c. 20-19 cal ka BP. Ice had retreated eastwards of this moraine by 17.9 cal ka BP. Hence formation of the moraine pre-dated the Killard Point Stadial readvance.
- The foraminiferal and sedimentological data indicate that glacimarine conditions, high relative sea level and cold waters prevailed during ice sheet retreat across the shelf. Evidence for retreat being driven by the advection of warm ocean water onto the shelf was not observed. Extensive zones of iceberg ploughmarks across the outer shelf imply that retreat was associated by a major phase of iceberg calving as the ice sheet stepped back from the shelf edge with glacimarine conditions, and thus high relative sea level, accompanying ice sheet retreat across the shelf.
- The data presented in this paper provide directly dated geomorphological and sedimentological evidence for a shelf-edge terminating, grounded BIIS at the LGM on the Atlantic shelf northwest of Ireland. Early retreat of the ice sheet in this sector during the gLGM eustatic lowstand was triggered by glacioisostasy and high relative sea level. This provides an explanation for the early retreat of the BIIS on the Atlantic shelf offshore Ireland and emphasises the importance of local relative sea-level rise driven by glacioisostatic crustal depression to initiate marine-based, ice sheet retreat.

Acknowledgements

This research was funded by the UK Natural Environment Research Council grant NE/J007196/1 'Britice-Chrono', and by the People Programme (Marie Curie Actions) of the European Union's Seventh Framework Programme FP7/2007–2013/under REA grant agreement no. 317217 ('GLANAM'). The work was supported by the NERC Radiocarbon Facility (Allocation No. 1722.0613 and 1878.1014). Thanks are due to the staff at the SUERC AMS Laboratory, East Kilbride for carbon isotope measurements. The CE08 research survey was carried out under the Sea Change Strategy with the support of the Irish Marine Institute and the Marine Research Sub-programme of the National Development Plan 2007–2013. We thank the officers and crew of the *RV Celtic Explorer* and the *RRS James Cook* for their help with data acquisition, the Geological Survey of Ireland for lending the vibrocorer for core acquisition during cruise CE08, the INFOMAR programme (www.infomar.ie) for additional funding to support cruise CE08, and the British Geological Survey for vibrocore collection during cruise JC106. Discussions with Professor Dave Roberts and comments on an earlier draft from Professor Chris Stokes helped to improve the manuscript and are gratefully acknowledged. We thank the reviewers, and particularly Dayton Dove for his insightful and thorough review.

Appendix A. Supplementary data

Supplementary data to this article can be found online at https://doi.org/10.1016/j.quascirev.2018.12.022.

References

Abe-Ouchi, A., Saito, F., Kawamura, K., Raymo, M.E., Okuno, J., Takahashi, K., Blatter, H., 2013. Insolation-driven 100,000-year glacial cycles and hysteresis of ice-sheet volume. Nature 500, 190–193.
Andrews, J.T., 1970. A Geomorphic Study of Postglacial Uplift with Particular Reference to Arctic Canada, vol. 2. Special Publication, London, England. Institute of British Geographers.
Andrews, J.T., 1987. The late Wisconsin glaciation and deglaciation of the laurentide ice sheet. In: Ruddiman, W.F., Wright Jr., H.E. (Eds.), North American and Adjacent Oceans during the Last Deglaciation, the Geology of North America, K-3. Geological Society of America, Boulder, Colorado, pp. 13–37.
Anderson, J.B., Brake, C.F., Myers, N.C., 1984. Sedimentation on the ross sea continental shelf, Antarctica. Mar. Geol. 57, 295–333.
Ashley, G., Smith, N., 2000. Marine sedimentation at a calving glacier margin. Geol. Soc. Am. Bull. 112 (5), 657–667.
Ballantyne, C.K., McCarroll, D., Stone, J.O., 2007. The Donegal ice dome, northwest Ireland: dimensions and chronology. J. Quat. Sci. 22, 773–783.
Ballantyne, C.K., Cofaigh, C., 2016. The last Irish Ice Sheet: extent and chronology. In: Coxon, P., McCarron, S., Mitchell, F., O'Connell, M. (Eds.), Advances in Quaternary Science: the Irish Quaternary, vol. 1. Atlantis Press, pp. 101–149.
Bamber, J., Alley, R., Joughin, I., 2007. Rapid response of modern day ice sheets to external forcing. Earth Planet. Sci. Lett. 257 (1), 1–13.
Bassis, J.N., Petersen, S.V., Mac Cathles, L., 2017. Heinrich events triggered by ocean forcing and modulated by isostatic adjustment. Nature 542, 332–334.
Batchelor, C.L., Dowdeswell, J.A., 2015. Ice-sheet grounding-zone wedges (GZWs) on high-latitude continental margins. Mar. Geol. 363, 65–92.
Benetti, S., Dunlop, P., Ó Cofaigh, C., 2010. Glacial and glacially-related features on the continental margin of northwest Ireland mapped from marine geophysical data. J. Maps 2010, 14–29.
Reconstruction of antarctic ice sheet deglaciation (RAISED). In: Bentley, M.J., Ó Cofaigh, C., Anderson, J.B. (Eds.), Quat. Sci. Rev. 100, 158.
Bowen, D.Q., Phillips, F.M., McCabe, A.M., Knutz, P.C., Sykes, G.A., 2002. New data on the last glacial maximum in great Britain and Ireland. Quat. Sci. Rev. 21, 89–101.
Bradwell, T., Stoker, M.S., Larter, R., 2007. Geomorphological signature and flow dynamics of the Minch palaeo-ice stream, NW Scotland. J. Quat. Sci. 22, 609–622.
Bradwell, T., Stoker, M.S., Golledge, N.R., Wilson, C.K., Merritt, J.W., Long, D., Everest, J., Hestvik, O.B., Stevenson, A.G., Hubbard, A.L., Finlayson, A., Mathers, H.E., 2008. The northern sector of the last British Ice Sheet: maximum extent and demise. Earth Sci. Rev. 88, 207–226.
Briner, J.P., Bini, A.C., Anderson, R.S., 2009. Rapid early Holocene retreat of a Laurentide outlet glacier through an Arctic fjord. Nat. Geosci. 2, 496–499.
Bronk Ramsey, C., 2009. Bayesian analysis of radiocarbon dates. Radiocarbon 51 (1), 337–360.
Callard, S.L., Ó Cofaigh, C., Benetti, S., Chiverrell, R.C., van Landeghem, K., Saher, M., Gales, J., Small, D., Clark, C.D., Livingstone, S.J., Fabel, D., 2018. Extent and retreat history of the Barra Fan Ice Stream offshore western Scotland and northern Ireland during the last glaciation. Quat. Sci. Rev. 201, 280–302.
Chiverrell, R.C., Thrasher, I.M., Thomas, G.S.P., Lang, A., Scourse, J.D., van Landeghem, K.J., McCarroll, D., Clark, C.D., Ó Cofaigh, C., Evans, D.J.A., Ballantyne, C.K., 2013. Bayesian modelling the retreat of the Irish Sea Ice stream. J. Quat. Sci. 28, 200–209.
Clark, C.D., Hughes, A.L.C., Greenwood, S.L., Jordan, C., Sejrup, H.P., 2012. Pattern and timing of retreat of the last British-Irish Ice Sheet. Quat. Sci. Rev. 44, 112–146.
Clark, J., McCabe, A., Schnabel, C., Clark, P.U., Freeman, S., Maden, C., Xu, S., 2009. ^{10}Be chronology of the last deglaciation of County Donegal, northwestern Ireland. Boreas 38 (1), 111–118.
Clark, P.U., Dyke, A.S., Shakun, J.D., et al., 2009. The last glacial maximum. Science 325, 710–714.
Conway, H., Hall, B.L., Denton, G.H., et al., 1999. Past and future grounding-line retreat of the west antarctic ice sheet. Science 286, 280–283.
Cowan, E.A., Cai, J., Powell, R.D., Clark, J.D., Pitcher, J.N., 1997. Temperate glacimarine varves: an example from Disenchantment Bay, southern Alaska. J. Sediment. Res. 67, 536–549.
Domack, E.W., 1984. Rhythmically bedded glaciomarine sediments on Whidey Island, Washington. J. Sediment. Petrol. 54, 589–602.
Domack, E., Harris, P.T., 1998. A new depositional model for ice shelves, based upon sediment cores from the Ross Sea and the Mac Robertson shelf, Antarctica. Ann. Glaciol. 27, 281–284.

Domack, E.W., Jacobson, E.A., Shipp, S., Anderson, J.B., 1999. Late Pleistocene-Holocene retreat of the west antarctic ice-sheet system in the ross sea: Part 2 - sedimentologic and stratigraphic signature. Geol. Soc. Am. Bull. 111, 1517–1536.
Dowdeswell, J.A., Whittington, R.J., Marienfeld, P., 1994. The origin of massive diamicton facies by iceberg rafting and scouring, Scores by Sund, East Greenland. Sedimentology 41, 21–35.
Dowdeswell, J.A., Fugelli, E.M.G., 2012. The seismic architecture and geometry of grounding-zone wedges formed at the marine margins of past ice sheets. Geol. Soc. Am. Bull. 124, 1750–1761.
Dowdeswell, J.A., Ottesen, D., Plassen, L., 2016. Debris-flow lobes on the distal flanks of terminal moraines in Sptisbergen fjords. In: Dowdeswell, J.A., Canals, M., Jakobsson, M., Todd, B.J., Dowdeswell, E.K., Hogan, K.A. (Eds.), Atlas of Submarine Glacial Landforms: Modern, Quaternary and Ancient. Geological Society, vol. 46. The Geological Society of London, London, pp. 77–78.
Dunlop, P., Shannon, R., McCabe, M., Quinn, R., Doyle, E., 2010. Marine geophysical evidence for ice sheet extension and recession on the Malin Shelf: new evidence for the western limits of the British Irish Ice Sheet. Mar. Geol. 276 (1), 86–99.
Dunlop, P., Sacchetti, F., Benetti, S., Ó Cofaigh, C., 2011. Mapping Ireland's glaciated continental margin using marine geophysical data. In: Smith, M.J., Paron, P., Griffiths, J.S. (Eds.), Geomorphological Mapping: Methods and Applications: A Professional Handbook of Techniques and Applications (Developments in Earth Surface Processes). Elsevier, pp. 337–355.
Elverhøi, A., Lønne, Ø., Seland, R., 1983. Glaciomarine sedimentation in a modern fjord environment, Spitsbergen. Polar Res. 1 (2), 127–150.
England, J.H., Furze, M.F.A., Doupe, J., 2009. Revision of the NW laurentide ice sheet: implications for paleoclimate, the northeast extremity of Beringia, and arctic ocean sedimentation. Quat. Sci. Rev. 28, 1573–1596.
Evans, D.J.A., Phillips, E.R., Hiemstra, J.F., Auton, C.A., 2006. Subglacial till: formation, sedimentary characteristics and classification. Earth Sci. Rev. 78, 115–176.
Evans, J., Pudsey, C.J., Ó Cofaigh, C., Morris, P., Domack, E., 2005. Late Quaternary glacial history, flow dynamics and sedimentation along the eastern margin of the Antarctic Peninsula Ice Sheet. Quat. Sci. Rev. 24 (5–6), 741–774.
Eyles, N., Eyles, C.H., Miall, A.D., 1983. Lithofacies types and vertical profile models: an alternative approach to the description and environmental interpretation of glacial diamict and diamictite sequences. Sedimentology 30 (3), 393–410.
Eyles, N., McCabe, A.M., 1989. The Late Devensian (22,000 BP) Irish Sea Basin: the sedimentary record of a collapsed ice sheet margin. Quat. Sci. Rev. 8, 307–351.
Eyles, C.H., Eyles, N., 2000. Subaqueous mass-flow origin for Lower Permian diamictites and associated facies of the Grant Group, Barbwire Terrace, Canning Basin, Western Australia. Sedimentology 47, 343–356.
Forwick, M., Vorren, T., 2011. Submarine mass wasting in isfjoren. In: Yamada, Spitsbergen, et al. (Eds.), Submarine Mass Movements and Their Consequences; Advances in Natural and Technological Hazards Research, vol. 31, pp. 711–722.
Gilbert, R., Aitken, A., Lemmen, D., 1993. The glacimarine sedimentary environment of expedition fiord, Canadian high arctic. Mar. Geol. 110 (3), 257–273.
Graham, A.G., Hodgson, D.A., 2016. Terminal moraines in the fjord basins of sub-Antarctic South Georgia. In: Dowdeswell, J.A., Canals, M., Jakobsson, M., Todd, B.J., Dowdeswell, E.K., Hogan, K.A. (Eds.), Atlas of Submarine Glacial Landforms: Modern, Quaternary and Ancient. Geological Society, vol. 46. The Geological Society of London, London, pp. 67–68.
Greenwood, S.L., Clark, C.D., 2009. Reconstructing the last Irish Ice Sheet 2: a geomorphologically-driven model of ice sheet growth, retreat and dynamics. Quat. Sci. Rev. 28, 3101–3123.
Hald, M., Korsun, S., 1997. Distribution of modern benthic foraminifera from fjords of Svalbard, European Arctic. J. Foraminifer. Res. 27 (2), 101–122.
Hemming, S.R., 2004. Heinrich events: massive late Pleistocene detritus layers of the North Atlantic and their global climate imprint. Rev. Geophys 42, RG1005. https://doi.org/10.1029/2003RG000128.
Hesse, R., Khodabakhsh, S., Klaucke, I., Ryan, W.B.F., 1997. Asymmetrical turbid surface-plume deposition near ice-outlets of the Pleistocene Laurentide ice sheet in the Labrador Sea. Geo Mar. Lett. 17, 179–187.
Hogan, K., Dowdeswell, J., Ó Cofaigh, C., 2012. Glacimarine sedimentary processes and depositional environments in an embayment fed by West Greenland ice streams. Mar. Geol. 311–314, 1–16.
Hogan, K., Ó Cofaigh, C., Jennings, A., Dowdeswell, J.A., Hiemstra, J., 2016. Deglaciation of a major palaeo-ice stream in Disko Trough, west Greenland. Quat. Sci. Rev. 147, 5–26.
Howe, J.A., 2006. Seabed morphology and the bottom-current pathways around rosemary bank seamount, northern Rockall Trough, North Atlantic. Mar. Petrol. Geol. 23, 165–181.
Howe, J.A., Stoker, M.S., Woolfe, K.J., 2001. Deep-marine seabed erosion and gravel lags in the northwestern Rockall Trough, North Atlantic ocean. J. Geol. Soc. 158, 427–438.
Hughes, T., 1987. Ice dynamics and deglaciation models when ice sheets collapsed. In: Ruddiman, W.F., Wright, H.E. (Eds.), North America and Adjacent Oceans during the Last Deglaciation, the Geology of North America, K-3. Geological Society of America, Boulder, Colorado, pp. 183–220.
Jamieson, S., Vieli, A., Livingstone, S.J., Ó Cofaigh, C., Stokes, C.R., Hillenbrand, C.-D., Dowdeswell, J.A., 2012. Ice stream stability on a reverse bed slope. Nat. Geosci. 5, 99–802.
Jennings, A.E., Hald, M., Smith, M., Andrews, J.T., 2006. Freshwater forcing from the Greenland Ice Sheet during the Younger Dryas: evidence from southeastern Greenland shelf cores. Quat. Sci. Rev. 25, 282–298, 2006.
Joughin, I., Smith, B.E., Medley, B., 2014. Marine ice sheet collapse potentially under way for the Thwaites Glacier Basin, West Antarctica. Science 344, 735–738.
Kilfeather, A.A., Ó Cofaigh, C., Lloyd, J.M., Dowdeswell, J.A., Xu, S., Moreton, S., 2011. Ice stream retreat and ice shelf history in Marguerite Bay, Antarctic Peninsula: sedimentological and foraminiferal signatures. Geol. Soc. Am. Bull. 123, 997–1015.
Korsun, S., Hald, M., 1998. Modern benthic foraminifera off Novaya Zemlya tidewater glaciers, Russian Arctic. Arct. Alp. Res. 30, 61–77.
Lambeck, K., Rouby, H., Purcell, A., Sun, Y., Sambridge, S., 2014. Sea Level and Global Ice Volumes from the Last Glacial Maximum to the Holocene. PNAS.
Lecavalier, B.S., Milne, G.A., Simpson, M.J., Wake, L., Huybrechts, P., Tarasov, L., Kjeldsen, K.K., Funder, S., Long, A.J., Woodroffe, S., Dyke, A.S., 2014. A model of Greenland ice sheet deglaciation constrained by observations of relative sea level and ice extent. Quat. Sci. Rev. 102, 54–84.
Livingstone, S.J., Cofaigh, C., Evans, D.J.A., 2010. A major ice drainage pathway of the last British-Irish Ice Sheet: the Tyne Gap, northern England. J. Quat. Sci. 25, 354–370.
Livingstone, S.J., Stokes, C.R., Ó Cofaigh, C., et al., 2016. Subglacial processes on an Antarctic ice stream bed 1: sediment transport and bedform genesis inferred from marine geophysical data. J. Glaciol. 62, 270–284. https://doi.org/10.1017/jog.2016.18.
Lloyd, J., 2006. Late Holocene environmental change in Disko Bugt, west Greenland: interaction between climate, ocean circulation and Jakobshavn Isbrae. Boreas 35, 35–49.
Lloyd, J., Park, L., Kuijpers, A., Moros, M., 2005. Early Holocene palaeoceanography and deglacial chronology of Disko Bugt, west Greenland. Quat. Sci. Rev. 24, 1741–1755.
Lønne, I., 1995. Sedimentary facies and depositional architecture of ice-contact glaciomarine systems. Sediment. Geol. 98, 13–43.
Lowe, D.R., 1982. Sediment gravity flows II. Depositional models with special reference to the deposits of high-density turbidity currents. J. Sediment. Petrol. 52, 279–297.
Mackiewicz, N., Powell, R., Carlson, P., Molnia, B., 1984. Interlaminated ice-proximal glacimarine sediments in Muir Inlet, Alaska. Mar. Geol. 57 (1–4), 113–147.
McCabe, A.M., Haynes, J.R., Macmillan, N.F., 1986. Late-Pleistocene tidewater glaciers and glaciomarine sequences from north County Mayo, Republic of Ireland. J. Quat. Sci. 1, 73–84.
McCabe, A.M., Clark, P., Clark, J., 2005. AMS 14C dating of deglacial events in the Irish Sea Basin and other sectors of the Britishelrish ice sheet. Quat. Sci. Rev. 24 (14), 1673–1690.
McCabe, A.M., Clark, P.U., Clark, J., 2007a. Radiocarbon constraints on the history of the western Irish ice sheet prior to the Last Glacial Maximum. Geology 35, 147–150.
McCabe, A.M., Clark, P.U., Clark, J., Dunlop, P., 2007b. Radiocarbon constraints on readvances of the British Irish Ice Sheet in the northern Irish Sea Basin during the last deglaciation. Quat. Sci. Rev. 26, 1204–1211.
McCarroll, D., 2001. Deglaciation of the Irish Sea Basin: a critique of the glaciomarine hypothesis. J. Quat. Sci. 16, 393–404.
Ó Cofaigh, C., Evans, D.J.A., 2001. Deforming bed conditions associated with a major ice stream of the last British ice sheet. Geology 29, 795–798.
Ó Cofaigh, C., Dowdeswell, J., 2001. Laminated sediments in glacimarine environments: diagnostic criteria for their interpretation. Quat. Sci. Rev. 20 (13), 1411–1436.
Ó Cofaigh, C., Larter, R.D., Dowdeswell, J.A., Hillenbrand, C.-D., Pudsey, C.J., Evans, J., Morris, P., 2005. Flow of the west antarctic ice sheet on the continental margin of the Bellingshausen sea at the last glacial maximum. J. Geophys. Res. 110 (11) https://doi.org/10.1029/2005JB003619.
Ó Cofaigh, C., Evans, J., Dowdeswell, J.A., Larter, R.D., 2007. Till characteristics, genesis and transport beneath Antarctic paleo-ice streams. J. Geophys. Res.: Earth Surfaces 112, F03006. https://doi.org/10.1029/2006JF000606.
Ó Cofaigh, C., Dunlop, P., Benetti, S., 2012. Marine geophysical evidence for Late Pleistocene ice sheet extent and recession on the continental shelf off northwest Ireland. Quat. Sci. Rev. 44, 147–159.
Ó Cofaigh, C., Dowdeswell, J., Jennings, A., Hogan, K., Kilfeather, A., Hiemstra, J., Noormets, R., Evans, J., McCarthy, D., Andrews, J., Lloyd, J., Moros, M., 2013. An extensive and dynamic ice sheet on the West Greenland shelf during the last glacial cycle. Geology 41 (2), 219–222.
Ó Cofaigh, C., Benetti, S., Dunlop, P., Monteys, X., 2016a. Arcuate moraines on the continental shelf northwest of Ireland. In: Dowdeswell, J.A., Canals, M., Jakobsson, M., Todd, B.J., Dowdeswell, E.K., Hogan, K.A. (Eds.), Atlas of Submarine Glacial Landforms: Modern, Quaternary and Ancient. Geological Society, vol. 46. The Geological Society of London, London, pp. 253–254.
Ó Cofaigh, C., Hogan, K., Dowdeswell, J.A., Streuff, K., 2016b. Stratified glacimarine basin-fills in West Greenland fjords. In: Dowdeswell, J.A., Canals, M., Jakobsson, M., Todd, B.J., Dowdeswell, E.K., Hogan, K.A. (Eds.), Atlas of Submarine Glacial Landforms: Modern, Quaternary and Ancient. Geological Society, vol. 46. The Geological Society of London, London, pp. 99–100.
Patton, H., Hubbard, A., Andreassen, K., Winsborrow, M., Stroeven, A.P., 2016. The build-up, configuration, and dynamical sensitivity of the Eurasian ice-sheet complex to Late Weichselian climatic and oceanic forcing. Quat. Sci. Rev. 153, 97–121.
Peters, J.E., Benetti, S., Dunlop, P., Ó Cofaigh, C., 2015. Maximum extent and dynamic behaviour of the last British-Irish Ice Sheet west of Ireland. Quat. Sci. Rev. 128, 48–68.

Peters, J.E., Benetti, S., Dunlop, P., Ó Cofaigh, C., Moreton, S.G., Wheller, A., Clark, C.D., 2016. Sedimentology and chronology of the advance and retreat of the last British-Irish Ice Sheet on the continental shelf west of Ireland. Quat. Sci. Rev. 140, 101–124.

Pfirman, S., Solheim, A., 1989. Subglacial meltwater discharge in the open-marine tidewater glacier environment: observations from Nordaustlandet, Svalbard archipelago. Mar. Geol. 86, 265–281.

Powell, R.D., 2003. Subaquatic landsystems: fjords. In: Evans, D.J.A. (Ed.), Glacial Landsystems. Arnold, London, pp. 313–347.

Powell, R.D., Domack, E.W., 1995. Modern glaciomarine environments. In: Menzies, J. (Ed.), Glacial Environments, vol. 1. Butterworth-Heinemann, Oxford, pp. 445–486. Modern Glacial Environments: Processes, Dynamics and Sediments.

Powell, R.D., Dawber, M., McInnes, J.N., Pyne, A.R., 1996. Observations of the grounding-line area at a floating glacier terminus. Ann. Glaciol. 22, 217–223.

Reimer, P.J., Bard, E., Bayliss, A., Beck, J.W., Blackwell, P.G., Bronk Ramsey, C., Grootes, P.M., Guilderson, T.P., Haflidason, H., Hajdas, I., Hatt, C., Heaton, T.J., Hoffmann, D.L., Hogg, A.G., Hughen, K.A., Kaiser, K.F., Kromer, B., Manning, S.W., Niu, M., Reimer, R.W., Richards, D.A., Scott, E.M., Southon, J.R., Staff, R.A., Turney, C.S.M., van der Plicht, J., 2013. IntCal13 and Marine13 radiocarbon age calibration curves 0-50,000 Years cal BP. Radiocarbon 55 (4), 1869–1887.

Rignot, E., Koppes, M., Velicogna, I., 2010. Rapid submarine melting of the calving faces of West Greenland glaciers. Nat. Geosci. 3 (3), 187–191.

Sacchetti, F., Benetti, S., Ó Cofaigh, C., Georgiopoulou, A., 2012. Geophysical evidence of deep-keeled icebergs on the Rockall bank, northeast atlantic ocean. Geomorphology 159–160, 63–72.

Scourse, J.D., Robinson, E., Evans, C.D.R., 1991. Glaciation of the central and southwestern Celtic Sea. In: Ehlers, J., Gibbard, P.L., Rose, J. (Eds.), Glacial Deposits in Great Britain and Ireland. Balkema, Rotterdam, pp. 301–310.

Scourse, J.D., Hall, I.R., McCave, I.N., Young, J.R., Sugdon, C., 2000. The origin of Heinrich layers: evidence from H2 for European precursor events. Earth Planet. Sci. Lett. 182, 187–195.

Scourse, J.D., Haapaniemi, A.I., Colmenero-Hidalgo, E., Peck, V.L., Hall, I.R., Austin, W.E.N., Knutz, P.C., Zahn, R., 2009. Growth, dynamics and deglaciation of the last British-Irish Ice Sheet: the deep-sea ice-rafted detritus record. Quat. Sci. Rev. 28, 3066–3084.

Sejrup, H.P., Clark, C.D., Hjelstuen, B.O., 2016. Rapid ice sheet retreat triggered by ice stream debuttressing: evidence from the North Sea. Geology 44, 355–358.

Small, D., Benetti, S., Dove, D., Ballantyne, C.K., Fabel, D., Clark, C.D., Gheorghiu, D.M., Newall, J., Xu, S., 2017. Cosmogenic exposure age constraints on deglaciation and flow behaviour of a marine-based ice stream in western Scotland, 21–16 ka. Quat. Sci. Rev. 167, 30–46.

Stoker, M.S., 1995. The influence of glacigenic sedimentation on slope-apron development on the continental margin off Northwest Britain. Geological Society, London, Special Publications 90 (1), 159–177.

Stokes, C.R., Corner, G.C., Winsborrow, M.C.M., Husum, K., Andreassen, K., 2014. Asynchronous response of marine-terminating outlet glaciers during deglaciation of the Fennoscandian Ice Sheet. Geology 42, 455–458.

Stroeven, A.P., Hättestrand, C., Kleman, J., Heyman, J., Fabel, D., Fredin, O., Goodfellow, B.W., Harbor, J.M., Jansen, J.D., Olsen, L., Caffee, M.W., Fink, D., Lundqvist, J., Rosqvist, G.C., Strömberg, B., Jansson, K., 2016. Deglaciation of fennoscandia. Quat. Sci. Rev. 147, 91–121.

Thomas, R., Frederick, E., Li, J., et al., 2011. Accelerating ice loss from the fastest Greenland and Antarctic glaciers. Geophys. Res. Lett. 38 (10).

Van Landeghem, K.J.J., Wheeler, A.J., Mitchell, N.C., 2009. Seafloor evidence for palaeo-ice streaming and calving of the grounded Irish Sea Ice Stream: implications for the interpretation of its final deglaciation phase. Boreas 38, 119–131.

Viana, A., Faugères, J.-C., Stow, D., 1998. Bottom-current-controlled sand deposits – a review of modern shallow-to deep-water environments. Sediment. Geol. 115, 53–80.

Walcott, R.I., 1970. Isostatic response to loading of the crust in Canada. Can. J. Earth Sci. 7, 716–726.

Walker, R.G., 1992. Turbidites and submarine fans. In: Walker, R.G., James, N.P. (Eds.), Facies Models: Response to Sea Level Change. Geological Association of Canada, pp. 239–263.

Wanamaker Jr., A.D., Butler, P.G., Scourse, J.D., Heinemeier, J., Eiríksson, J., Knudsen, K.L., Richardson, C.A., 2012. Surface changes in the North Atlantic meridional overturning circulation during the last millennium. Nat. Commun. 3, 899. https://doi.org/10.1038/ncomms1901.

Whittington, R.J., Niessen, F., 1997. A cross-section of a fjord debris flow, East Greenland. In: Davies, T.A. (Ed.), Glaciated Continental Margins: an Atlas of Acoustic Images. Chapman and Hall, New York, pp. 128–129.